

# 1 **Isotopic variations in surface waters and groundwaters of an extremely arid** 2 **basin and their responses to climate change**

3 Yu Zhang<sup>1</sup>, Hongbing Tan<sup>1,\*</sup>, Peixin Cong<sup>1</sup>, Dongping Shi<sup>1</sup>, Wenbo Rao<sup>1</sup>, Xiying Zhang<sup>2</sup>

4 <sup>1</sup>School of Earth Sciences and Engineering, Hohai University, Nanjing 210098, China

5 <sup>2</sup>Qinghai Institute of Salt Lakes, CAS, Xining 810008, China

6 **\* Corresponding author:** Hongbing Tan (tan815@sina.com)

## 7 **Abstract**

8 Climate change accelerates the global water cycle. However, the relationships between  
9 climate change and hydrological processes in the alpine arid regions remain elusive. We sampled  
10 surface water and groundwater at high spatial and temporal resolution to investigate these  
11 relationships in the Qaidam Basin, an extremely arid area in the northeastern Tibetan Plateau.  
12 Stable H-O isotopes and radioactive <sup>3</sup>H isotope were combined with atmospheric simulations to  
13 examine hydrological processes and their response mechanisms to climate change. Contemporary  
14 climate processes and change dominate the spatial and temporal variations of surface water  
15 isotopes, specifically, the westerlies moisture transport and the local temperature and precipitation  
16 regimes. The ~~spatial~~-H-O isotopic compositions in the Eastern Kunlun Mountains showed a  
17 gradually depleted eastward pattern; while a reverse pattern occurred in the Qilian Mountains  
18 water system. Precipitation contributed significantly more to river discharge in the eastern basin  
19 (approximately 45%) than in the middle and western basin (10%–15%). Moreover, increasing  
20 precipitation and shrinking cryosphere caused by current climate change have accelerated basin  
21 groundwater circulation. In the eastern and southwestern Qaidam Basin, precipitation and  
22 meltwater infiltrate along preferential flow paths, such as faults, volcanic channels, and fissures,  
23 permitting rapid seasonal groundwater recharge and enhanced terrestrial water storage. However,  
24 compensating for water loss due to long-term ice and snow melt will be a challenge under projected  
25 increasing precipitation in the southwestern Qaidam Basin, and the total water storage may show  
26 a trend of increasing before decreasing. Great uncertainty about water is a potential climate change  
27 risk facing the arid Qaidam Basin.

## 28 **1. Introduction**

29 In the face of ongoing environmental changes, a thorough understanding of the hydrological  
30 cycle is a prerequisite for accurate trend forecasting, and helps to design efficient water resource  
31 management strategies. Over the past half century, climate change and more intense human  
32 activities have led to global water cycle acceleration and water resource redistribution at different  
33 scales (Huntington et al., 2006; Durack et al., 2012; Masson-Delmotte et al., 2021). For example,  
34 rapid warming has sharply expanded lakes in the Tibetan Plateau and shrunk them in the  
35 Mongolian Plateau (Zhang et al., 2017), and has also exacerbated the severe irrigation water  
36 shortage in parts of South Asia and East Asia (Haddeland et al., 2014). Moreover, warming is  
37 expected to reduce groundwater storage in the western United States (Condon et al., 2020).  
38 Currently, the climate in arid regions of northwestern China is changing from warm–dry to warm–  
39 wet (Zhang et al., 2021). The resulting uncertainties in water resources in arid alpine basins pose  
40 new challenges to understand the hydrological cycle and water resources. These key scientific  
41 issues can be addressed by investigating the spatial and temporal distribution and control  
42 mechanisms of surface water and groundwater resources within the basin under accelerating  
43 climate change.

44 The Tibetan Plateau, known as the “Third Pole”, has complex cryospheric-hydrologic-  
45 geodynamic processes and is especially vulnerable to global warming (Zhang et al., 2017; Yao et  
46 al., 2022). The Qaidam Basin in the northeastern Tibetan Plateau is the area that has warmed the  
47 most in the entire Tibetan Plateau (Li et al., 2015; Kuang and Jiao, 2016; Yao et al., 2022). Since  
48 1961, the average temperature of the basin has increased at an alarming rate of 0.53°C per decade  
49 (Wang et al., 2014), resulting in increased precipitation and cryospheric retreat (Song et al., 2014;  
50 Xiang et al., 2016; Zou et al., 2022; Wang et al., 2023). These changes have led to drastic spatial  
51 changes in surface water and groundwater storage, increasing runoff over wide areas (Jiao et al.,  
52 2015; Wei et al., 2021), and hydrological changes in the central and northern basin, such as the  
53 lakes expansion (Ke et al., 2022; Zhang et al., 2022). However, several questions remain to be  
54 answered: How are hydrological changes in the basin driven by climate change? What are the  
55 potential influences of these changes on the water resources of the basin? The dynamics of surface  
56 water and groundwater, which link precipitation and meltwater from high elevations with the low-  
57 lying lake basins, provide evidence of the effects of climate change on water cycle processes. The

58 Qaidam Basin is therefore an excellent site to reveal the mechanisms of global warming-induced  
59 responses to the hydrological cycle on the Tibetan Plateau.

60 The isotopes of hydrogen and oxygen are useful tracers for the water cycle and climate  
61 reconstruction. They can help elucidate the processes that control water cycle changes, thus  
62 providing scientific evidence for human adaptations and effects on future global changes (Craig,  
63 1961; Dansgaard, 1964; Yao et al., 2013; Bowen et al., 2019; Kong et al., 2019; Zhu et al., 2023).  
64 Water isotope records provide key information on water flow, and they can compensate for the  
65 paucity of hydrometeorological, geological, and borehole data in hydrological research. Stable H-  
66 O isotopes and radioactive  $^3\text{H}$  isotope have been widely applied to quantify surface water or  
67 groundwater recharge sources, interactions, budgets, and ages (Befus et al., 2017; Stewart et al.,  
68 2017; Moran et al., 2019; Bam et al., 2020; Rodriguez et al., 2021; Shi et al., 2021; Ahmed et al.,  
69 2022; Benettin et al., 2022). Previous researchers have also performed a substantial amount of  
70 work on using isotopes to delineate the water cycle in the Qaidam Basin (Xu et al., 2017; Xiao et  
71 al., 2017, 2018; Zhao et al., 2018; Tan et al., 2021; Yang and Wang, 2020; Yang et al., 2021).  
72 These studies have enhanced our understanding of aquifer properties in local regions and recharge  
73 mechanisms. However, past assessments of the water cycle in the Qaidam Basin have been  
74 constrained by the challenges of the harsh natural conditions and scarce hydrogeological data. It is  
75 a great challenge to achieve a comprehensive elucidation of the basin-scale water cycle mechanism.  
76 Furthermore, seasonal recharge of the whole basin has not been systematically explored. Various  
77 hydrological, climatic, and hydrogeological conditions of the basin are caused by continuous  
78 changes in the topographical and tectonic spatial patterns; moreover, the hydrological effects  
79 exerted by anthropogenic climate change differ seasonally (Jasechko et al., 2014). Therefore, it is  
80 urgent to develop a comprehensive understanding of the basin water cycle and its seasonal changes.  
81 While carrying out a comprehensive assessment of differences in isotopic compositions of various  
82 potential recharge sources, it is fundamental to use the same technical methods for the systematic  
83 sampling and isotopic characterization of the basin.

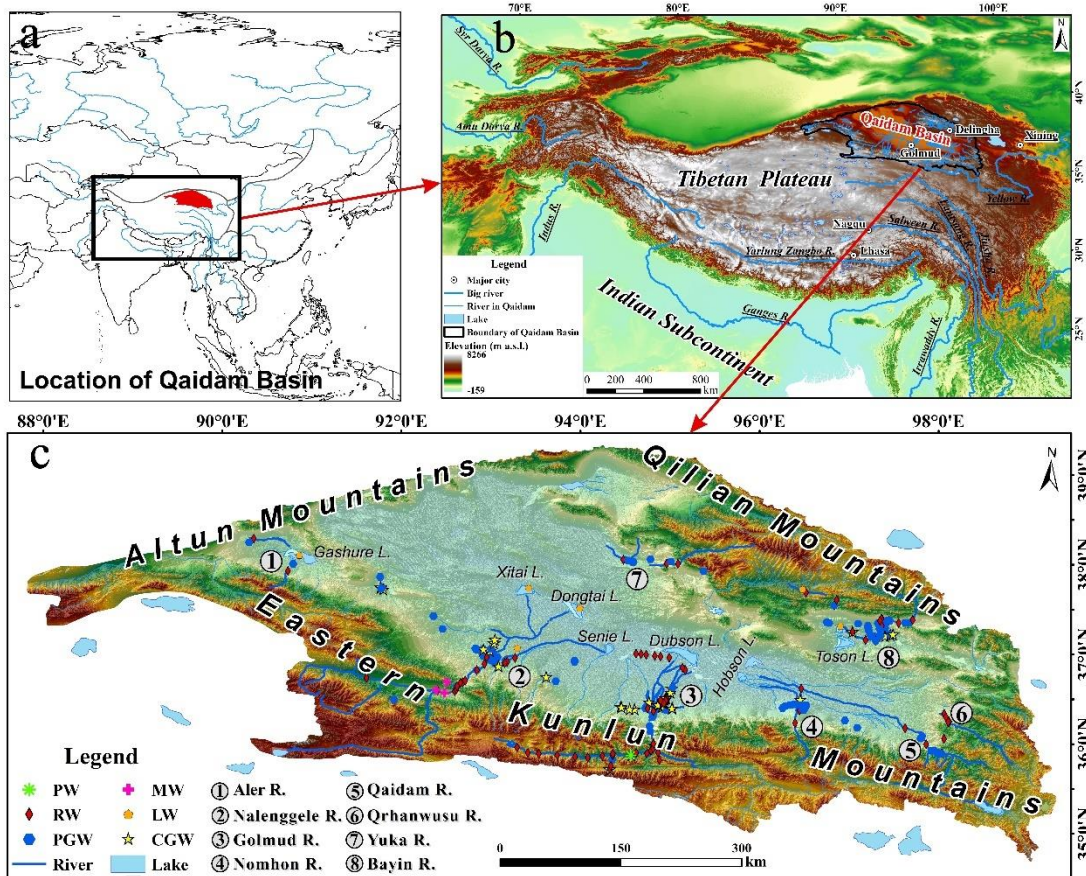
84 In this study, we constrain the hydrological cycle of the Qaidam Basin and surrounding  
85 mountains using stable H-O and radioactive  $^3\text{H}$  isotope data collected during the wet and dry  
86 seasons from eight study sites in major watersheds in the basin. The study aims are: 1) to elucidate  
87 the distribution pattern of surface water and groundwater isotopes in this alpine arid basin at  
88 various spatial and seasonal scales; 2) to identify and quantify the main components of the regional

89 water cycle, their timing and spatial heterogeneity; and 3) to reveal isotopic hydrological responses  
90 to climate change and to predict the trend of the changes of Qaidam Basin water resources.

## 91 **2. Study area**

### 92 2.1. General features

93 The Qaidam Basin is a closed fault-depression basin in the northeastern Tibetan Plateau  
94 surrounded by the Kunlun, Qilian and Altun Mountains (Figures 1a and 1b). The basin is one of  
95 the four main basins in China with an area of approximately 250,000 km<sup>2</sup>. It has a plateau  
96 continental climate with a typical alpine arid inland basin characterized by drought. There are  
97 significant temperature variations across the basin, and the mean annual temperature is less than  
98 5 °C. Annual precipitation varies from 200 mm in the southeastern region to 15 mm in the  
99 northwestern region. Mean annual relative humidity is 30%–40%, with a minimum of less than  
100 5%. Modern glaciers have formed in the mountains on the western, southern and northeastern sides  
101 of the basin. The basin is surrounded by more than 100 rivers, about 10 rivers of which are  
102 perennial, with most of the local rivers being intermittent river systems. The rivers are mainly  
103 distributed on the eastern side of the basin but are scarce on the western side. The water in the  
104 basin's lakes is predominantly saline, with a total of 31 salt lakes.



105

106 **Figure 1.** Location of Qaidam Basin (a, b) and the sampling sites (c).

107 **2.2 Basic hydrogeological setting**

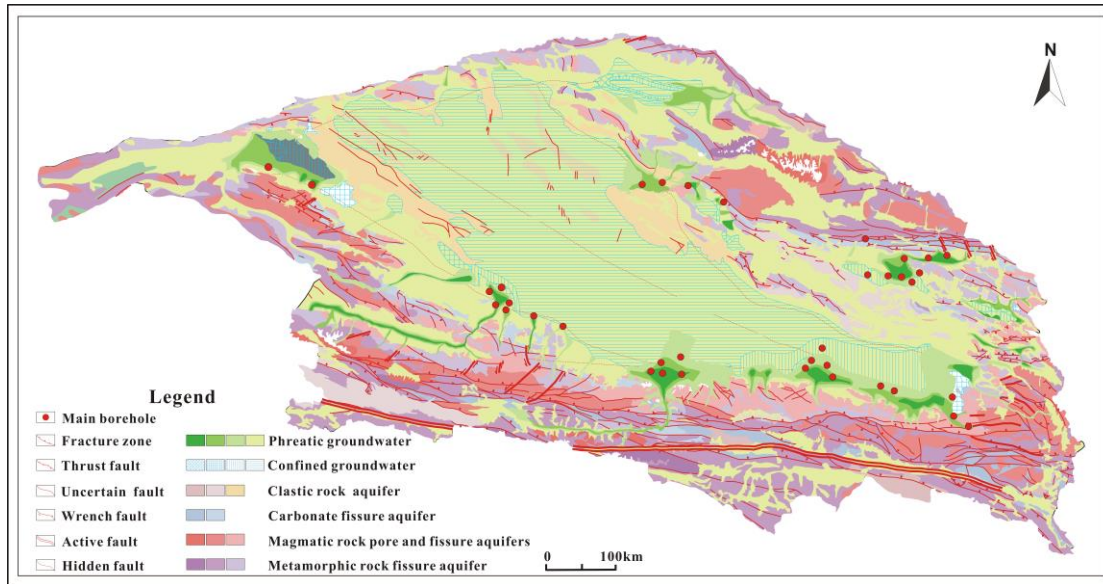
108 The basin basement consists of Precambrian crystalline metamorphic rock series, and the  
 109 caprock is of Paleogene-Neogene and Quaternary strata. The mountainous area surrounding the  
 110 basin is dominated by a Paleogene system, and the basin area and basin boundary zone are  
 111 characterized by a wide distribution of the Paleogene-Neogene system. The Quaternary system is  
 112 mainly distributed in the central basin region and the intermountain valley region. The basin terrain  
 113 is slightly tilted from the northwest to southeast, and the height gradually reduces from 3000 m to  
 114 approximately 2600 m. The distribution of the basin landforms shows a concentric ring shape.  
 115 From the rim to the centre, the distribution of diluvial gravel fan (Gobi), alluvial–diluvial silt plain,  
 116 lacustrine–alluvial silt clay plain, and lacustrine silt–salt plains follow a regular pattern. Salt lakes  
 117 are extensively distributed in the lowlands. The inner edge of the Gobi belt in the northwestern  
 118 basin region is clustered with hills that are less than 100 m in height. The southeastern region of

119 the basin has pronounced subsidence, and the alluvial and lacustrine plains are extensive. In the  
120 northeastern basin, a secondary small intermountain basin has been formed between the basin and  
121 the Qilian Mountains by the uplifting of a series of low mountain fault blocks of metamorphic rock  
122 series.

123 The Qaidam Basin is located in the Qin-Qi-Kun tectonic system, where there is strong  
124 neotectonic movement, and a series of syncline-anticline tectonic belts and regional deep faults  
125 have formed around it. The fault structures in the Qaidam Basin are very well developed and  
126 include the north-easterly Altun fault in the north; north-westerly Saishenteng–Aimunik northern  
127 margin deep fault in the northeast; westerly Qaidam northern margin deep fault in the northwest;  
128 Qimantag Mountains and Burhan Budai Mountains–Aimunik northern margin deep fault in the  
129 south; and north-westerly Sanhu major fault and north-easterly Qigaisu–Dongku Fault in the  
130 central basin region.

131 The distribution of surface water in the basin is constrained by topography and neotectonic  
132 movements and appears to have a general centripetal radial pattern (Figure 1c). There is  
133 widespread surface water and groundwater exchange. The mountainous areas are rich in  
134 precipitation and ice/snow meltwater, and are the main runoff producing areas. Runoff from the  
135 mountains flows through the Gobi belt, where most of it infiltrates into the groundwater system.  
136 Groundwater discharges to the surface from springs in confined aquifers or springs at the front  
137 edge of the alluvial fan. This water finally flows into terminal lakes.

138 Groundwater can be roughly classified as: i) fractured-bedrock water; ii) leached pore water  
139 and local confined groundwater; iii) phreatic groundwater and confined artesian water; iv) saline  
140 phreatic groundwater; v) brine, and saline confined artesian water. Surface water and groundwater  
141 salinity and solutes are gradually enriched along the flow path (Figure 2; Wang et al., 2008).



142

143 **Figure 2.** Hydrogeologic map of the Qaidam Basin (Modified from Xi'an Center, China Geological Survey,  
 144 <http://www.xian.cgs.gov.cn/>). The color of different patches of the same aquifer, from dark to light, denotes high  
 145 to low in water yield property.

### 146 3. Sampling and methods

#### 147 3.1 Sampling and analysis

148 We collected samples from 8 major river–groundwater systems in the region from 2019 to  
 149 2021. We collected samples from 6 of the systems once a hydrological year, consisting of the wet  
 150 season (July–August) and the dry season (March–April). Precipitation and snow meltwater were  
 151 collected from the Eastern Kunlun Mountains. Snow meltwater was collected in the dry season  
 152 whereas precipitation was collected at several times during a hydrological year. In total, 239  
 153 sampling points were established: phreatic groundwater (n = 100), confined groundwater (n = 43),  
 154 spring water (n = 6), river water (n = 81), lake water (n = 5), snow meltwater (n = 3), and  
 155 precipitation (n= 1). A total of 422 sets of samples were collected. No sampling point was  
 156 established in the northwestern basin because the southern slope and front edge of the Altun  
 157 Mountains consisted of Tertiary system halite sedimentation and Quaternary system thick salt flats,  
 158 and no freshwater body was developed. Therefore, the sample collection covers the entire Qaidam  
 159 Basin and each of the major endorheic regions.

160 Hydrogen and oxygen isotopes ( $^2\text{H}$ ,  $^3\text{H}$ , and  $^{18}\text{O}$ ) were analyzed at the State Key Laboratory  
161 of Hydrology-Water Resources and Hydraulic Engineering, Hohai University, China. A MAT253  
162 mass spectrometer was used to measure the ratios of  $^2\text{H}/^1\text{H}$  and  $^{18}\text{O}/^{16}\text{O}$ , and the results were  
163 compared with the Vienna Standard Mean Ocean Water (VSMOW), expressed in  $\delta$  (‰), with the  
164 analytical precision ( $1\sigma$ ) of the instrument for these isotopes was lower than  $\pm 1\%$  and  $\pm 0.1\%$ . To  
165 determine the tritium ( $^3\text{H}$ ) concentration, the water sample was first concentrated by electrolysis.  
166 Following sample enrichment, measurements were carried out using low background liquid  
167 scintillation counting (TRI-CARB 3170 TR/SL). The findings were expressed in terms of absolute  
168 concentration in tritium units (TU), the detection limit of the instrument was 0.2 TU, and the  
169 precision was improved to less than  $\pm 0.8$  TU.

### 170 3.2 Hydrograph separation

171 In the analysis of water sources among hydrological processes, endmember mixing models  
172 are widely used. The contribution of each recharge endmember to the mixed water body was  
173 estimated with a Bayesian mixing model that considers to the heterogeneity of different  
174 endmember isotopes/water chemistry parameters (Hooper et al., 1990, 2003; Chang et al., 2018).  
175 The process is as follows:

$$176 \quad 1 = \sum_{i=1}^n f_i, \quad C_m^j = \sum_{i=1}^n f_i C_i^j, \quad j = 1, \dots, n \quad (1)$$

177 where  $f_i$  represents the proportion of water source  $i$ ,  $n$  represents the number of endmembers, and  
178  $C_m^j$  represents the level of tracer  $j$  in endmember  $i$ .

179 The Bayesian mixing models (MixSIAR) coded in R can quantify the contributions of more  
180 than two potential endmembers (Parnell et al., 2010). In this study, based on the differences in the  
181 water body properties and isotopic composition of each endmember,  $\delta^{18}\text{O}$ ,  $\delta\text{D}$ , and d-excess (d-  
182 excess =  $\delta\text{D} - 8\delta^{18}\text{O}$ ) data were used as parameters in the modeling. The model was calculated at  
183 a fractional increment of 1% and an uncertainty level of 0.1%.

### 184 3.3 Water vapor trajectory

185 The source and transport route of moisture can be monitored based on the water vapor flux  
186 field derived from the monthly mean ERA5 reanalysis data ( $0.25^\circ \times 0.25^\circ$ ) of the European Centre

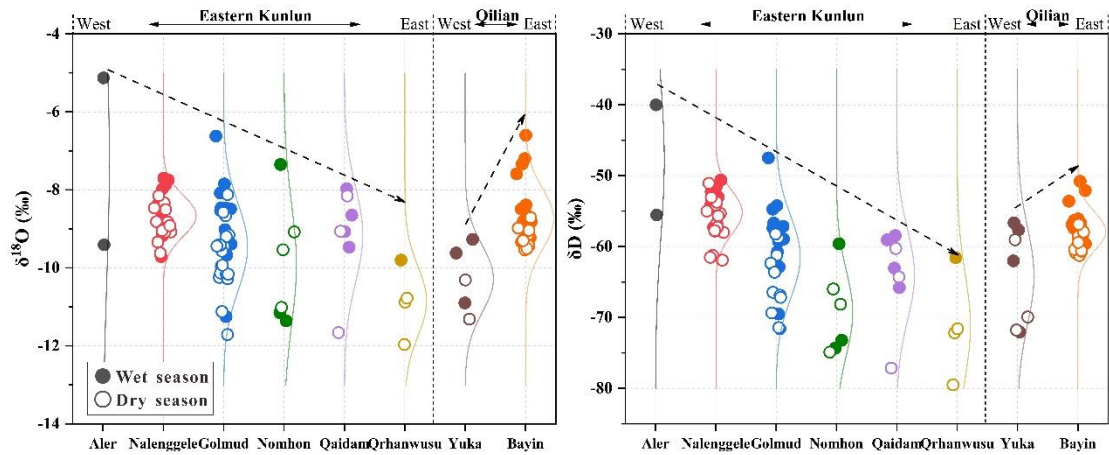


187 for Medium-Range Weather Forecasts (ECMWF, <https://www.ecmwf.int/>) (Hersbach et al., 2019).  
188 After taking into account that more than 70% of the precipitation in the Qaidam Basin occurs from  
189 June to September, the monthly mean ERA5 reanalysis data in this period from 2019 to 2021 were  
190 used to analyze the water vapor transport path in and around the study area. Based on the average  
191 altitude of >3000 m at the study site, the simulated atmospheric pressure was set to 500 hPa. The  
192 majority of the atmospheric water vapor was distributed in the range of 0–2 km above ground, and  
193 the simulated height did not have any significant influence on the findings (Li and Garzione, 2017;  
194 Yang and Wang, 2020).

## 195 **4. Results**

### 196 4.1 Spatial and seasonal characteristics of surface water $\delta^{18}\text{O}$ - $\delta\text{D}$

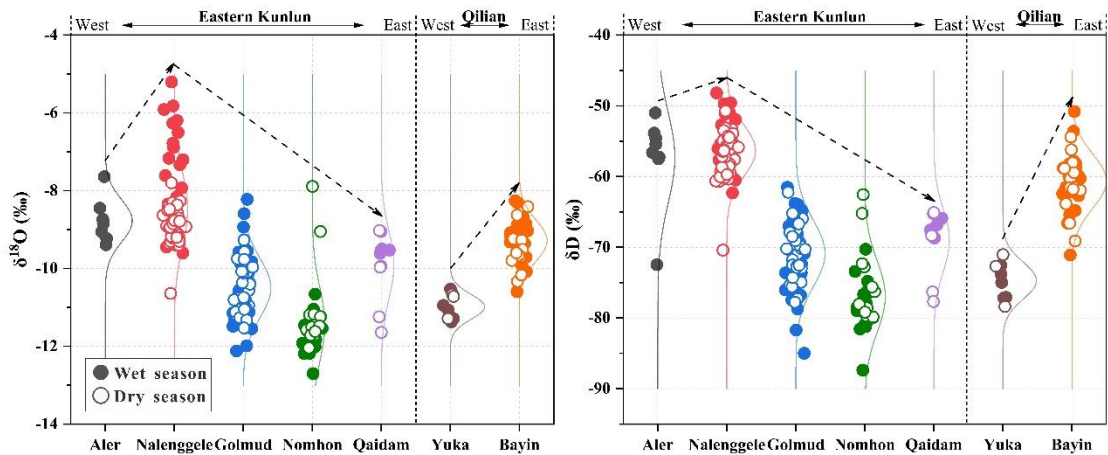
197 In the Qaidam Basin, considerable spatial and seasonal variations exist in the stable H-O  
198 isotopes of surface water (Figure 3). The isotopic compositions of rivers originating from the  
199 Eastern Kunlun Mountains contrast with those from Qilian Mountains, where the heavy isotopes  
200 of the Eastern Kunlun Mountains are gradually depleted in the direction of west to east, and the  
201 reverse holds true for the Qilian Mountains. Of these, the  $\delta^{18}\text{O}$  and  $\delta\text{D}$  values are significantly  
202 positive in the southwestern basin, while significantly negative in the eastern basin. Apart from  
203 the Nomhon River, all watersheds exhibit a characteristic seasonal variation of enriched in heavy  
204 isotope during the wet season relative to the dry season. The mean  $\delta^{18}\text{O}$  and  $\delta\text{D}$  values in surface  
205 water are more positive by  $-0.08\text{‰}$  to  $1.08\text{‰}$  and  $0.6\text{‰}$  to  $10.6\text{‰}$ , respectively, in the wet season.  
206 Moreover, the seasonal variations of  $\delta^{18}\text{O}$  and  $\delta\text{D}$  are more evident in the downstream river  
207 compared to the upstream. For instance, the  $\delta^{18}\text{O}$  value of the downstream Nomhon River is  $3.66\text{‰}$   
208 higher during the wet season compared to the dry season. These phenomena reflect the differences  
209 in the recharge sources of the river during both the wet and dry seasons and the strong evaporation  
210 effect in the central basin region.



211  
 212 **Figure 3.** Spatial and temporal variation in the H-O isotope composition of Qaidam Basin river water. Filled  
 213 and hollow dots indicate wet and dry seasons, respectively; The light-dashed lines indicate the trend of  $\delta^{18}\text{O}$  and  
 214  $\delta\text{D}$  from west to east.

215 4.2 Spatial and seasonal characteristics of groundwater  $\delta^{18}\text{O}$ - $\delta\text{D}$

216 The spatial variability of groundwater stable H-O isotopes is more pronounced compared with  
 217 river water, although it appears to follow the same distribution pattern as river water in the basin  
 218 (Figure 4). The  $\delta^{18}\text{O}$  and  $\delta\text{D}$  values in groundwater system are lower and seasonal fluctuations  
 219 were smaller compared to those in surface water because the kinetic fractionation of isotopes  
 220 caused by evaporation and mixing are weaker in groundwater than in surface water. Specifically,  
 221 the average seasonal variation of  $\delta^{18}\text{O}$  in each of the groundwater systems ranges from  $-0.75\text{‰}$  to  
 222  $+0.84\text{‰}$ , and the largest seasonal variations in individual boreholes are  $+3.31\text{‰}$  and  $-3.16\text{‰}$ ,  
 223 respectively. This suggests that the groundwater reflects a spatial and temporal average of the  
 224 surface water isotopic signal, and averaging reduces the variability of the values. The region with  
 225 the greatest seasonal fluctuations of groundwater is located in the Nalenggele River, southwestern  
 226 basin, and the groundwater  $\delta^{18}\text{O}$  and  $\delta\text{D}$  in wet season are noticeably more positive compared to  
 227 those in dry season. This indicates that groundwater is flowing rapidly and each season, new  
 228 infiltration displaces the earlier infiltration. The adjacent Golmud River, however, has the least  
 229 seasonal variations in  $\delta^{18}\text{O}$  and  $\delta\text{D}$ . In contrast, this suggests that flow is slow. Although there are  
 230 no obvious differences in the topography and landforms between the two adjacent watersheds,  
 231 significant differences are observed in the isotope signatures of the two, where both surface water  
 232 and groundwater show much more positive  $\delta^{18}\text{O}$  and  $\delta\text{D}$  values in the Nalenggele River than that  
 233 of Golmud River catchment.



234

235 **Figure 4.** Spatial and temporal variation in H-O isotopes in the groundwater of the Qaidam Basin. Filled and  
 236 hollow dots indicate wet and dry seasons, respectively; The light-dashed lines indicate the trend of  $\delta^{18}\text{O}$  and  $\delta\text{D}$   
 237 from west to east.

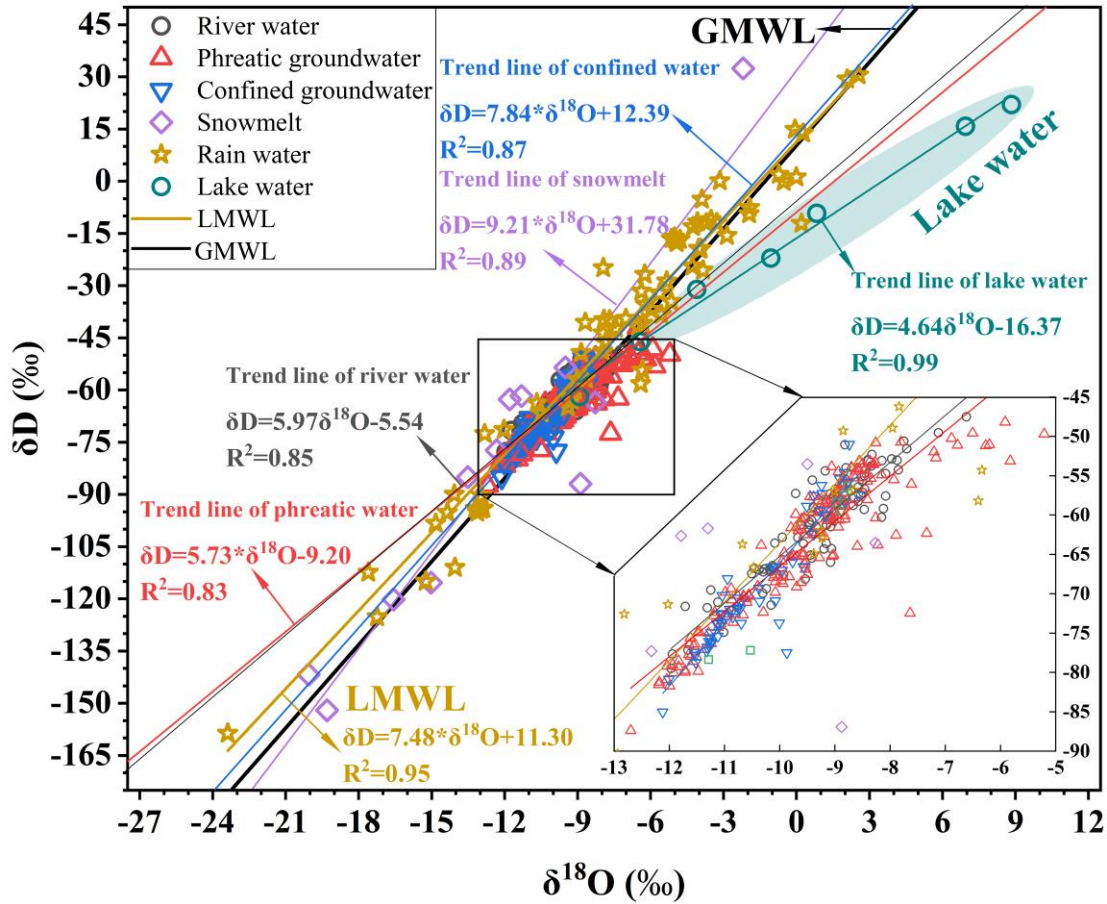
### 238 4.3 Isotopic variations in different water bodies

239 In the Qaidam Basin, the ranges of  $\delta^{18}\text{O}$  and  $\delta\text{D}$  of the precipitation samples from the Kunlun  
 240 Mountains and Qilian Mountains are  $-23.38\text{‰}$  to  $+2.55\text{‰}$  and  $-158.6\text{‰}$  to  $+30.5\text{‰}$ , respectively  
 241 (Table S1; Zhu et al., 2015). The fitted local meteoric water line (LMWL) equation in the Qaidam  
 242 Basin is  $\delta\text{D} = 7.48\delta^{18}\text{O} + 11.30$  ( $R^2 = 0.95$ ,  $n = 74$ ), where the slope and intercept are similar to  
 243 the long-term monitoring findings of the Qilian Mountains (Figure 5; Zhao et al., 2011; Juan et al.,  
 244 2020; Wu et al., 2022; Yang et al., 2023). In the Qaidam Basin, the heavy isotopes present in snow  
 245 meltwater samples are considerably depleted compared to rainwater (Clark and Fritz, [2013](#)[1997](#)).  
 246 The  $\delta^{18}\text{O}$  and  $\delta\text{D}$  ranges are  $-19.30\text{‰}$  to  $-2.19\text{‰}$  and  $-152.0\text{‰}$  to  $32.4\text{‰}$  respectively, and the  
 247 fitting trend equation was  $\delta\text{D} = 9.21\delta^{18}\text{O} + 31.78$  ( $R^2 = 0.89$ ,  $n = 12$ ), with the slope and intercept  
 248 greater than LMWL and GMWL (Global meteoric water line).

249 The  $\delta^{18}\text{O}$  and  $\delta\text{D}$  ranges in river water are  $-13.51\text{‰}$  to  $-5.93\text{‰}$  and  $-85.0\text{‰}$  to  $-47.5\text{‰}$   
 250 respectively, whereas those in the lake water are more enriched at  $-4.10\text{‰}$  to  $8.84\text{‰}$  and  $-31.1\text{‰}$   
 251 to  $22.1\text{‰}$ , respectively (Figure 5). The fitted trend lines for river and lake samples are:  $\delta\text{D} =$   
 252  $5.97\delta^{18}\text{O} - 5.54$  ( $R^2 = 0.85$ ,  $n = 92$ ) and  $\delta\text{D} = 4.64\delta^{18}\text{O} - 16.37$  ( $R^2 = 0.99$ ,  $n = 7$ ), respectively,  
 253 which are below both the GMWL and LMWL, indicating varying extents of evaporative  
 254 fractionation in the surface water bodies, with evaporation from lakes being more enhanced. The  
 255 radioactive  $^3\text{H}$  concentrations range from 4.2 to 17.8 TU, with a mean value of 12.93 TU ( $n=23$ ,  
 256 Table S1).

257 The H-O isotopic composition ranges in the groundwater samples are wider and considerable  
258 differences are observed between phreatic and confined groundwater (Figure 5). The  $\delta^{18}\text{O}$  and  $\delta\text{D}$   
259 values range in phreatic groundwater from  $-12.70\text{‰}$  to  $-5.21\text{‰}$  and  $-87.4\text{‰}$  to  $-42.0\text{‰}$ ,  
260 respectively. The fitted trend line is  $\delta\text{D} = 5.73\delta^{18}\text{O} - 9.20$  ( $R^2 = 0.83$ ,  $n = 185$ ). The phreatic  
261 groundwater isotopic composition and slope of the trend line are similar to those of surface water,  
262 indicating considerable interactions between the two and substantial evaporative fractionation of  
263 some shallow groundwater. The  $\delta^{18}\text{O}$  and  $\delta\text{D}$  ranges in confined groundwater are relatively small  
264 and lower in comparison at  $-12.12\text{‰}$  to  $-8.58\text{‰}$  and  $-85.0\text{‰}$  to  $-51.0\text{‰}$ . The linear regression  
265 relationship of the samples fitting ( $\delta\text{D} = 7.84\delta^{18}\text{O} + 12.39$ ,  $R^2 = 0.87$ ,  $n = 51$ ) revealed that its  
266 slope and intercept were essentially consistent with those of GMWL and LMWL, suggesting the  
267 presence of a strong correlation between confined groundwater and atmospheric precipitation in  
268 different periods. Radioactive  $^3\text{H}$  concentrations detectable in the phreatic and confined  
269 groundwater range from 0.22 to 30.35 TU and 0.60 to 12.76 TU, respectively, with mean values  
270 of 10.23 TU ( $n=49$ ) and 7.55 TU ( $n=10$ ), respectively (Table S1).

271 Overall, the stable H-O isotopic compositions of surface water and groundwater are generally  
272 more enriched in the Qaidam Basin. The isotopic compositions and trend fitting features both  
273 demonstrated that the water samples have undergone varying degrees of evaporation during runoff,  
274 indicating the cold and dry climate environmental characteristics of the study area.



275

276 **Figure 5.** Plot of the relationships between  $\delta^{18}\text{O}$  and  $\delta\text{D}$  in different water bodies from the Qaidam Basin.

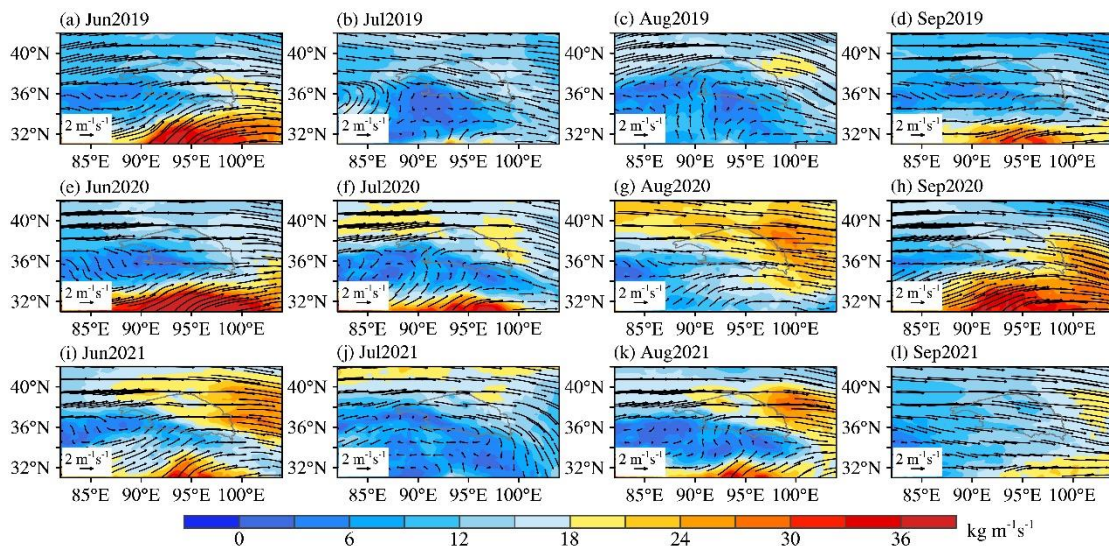
277 **5. Discussion**

278 5.1 Water cycle information indicated by surface water isotopes

279 5.1.1 Atmospheric moisture transport pattern

280 To further explain the cause of spatial and seasonal variations of surface water  $\delta^{18}\text{O}$  and  $\delta\text{D}$   
 281 values, ERA5 reanalysis data in the rainy season (June to September) were used to calculate the  
 282 water vapor flux field in the Qaidam Basin and its surrounding areas as well as track the main  
 283 trajectories of the moisture transport (Hersbach et al., 2019). The results show that the mid-latitude  
 284 westerlies dominate the moisture paths inside and around the basin, and the water vapor flux in  
 285 the eastern basin is notably greater than that in the western basin (Figure 6; Yang and Wang, 2020).  
 286 This largely explains the spatial patterns of river water H-O isotopes (Figure 3), as well as  
 287 temperature and precipitation regimes (Figure S1). Atmospheric and isotopic tracing data also  
 288 support these conclusions. For instance, the Tanggula Mountains ( $33^{\circ}$ – $35^{\circ}$  N) serve as the physical

289 and chemical boundary of the Tibetan Plateau, and the westerlies fundamentally govern the  
 290 northern region, preventing the Indian monsoon from having a significant impact on the Qaidam  
 291 Basin (Yao et al., 2013; Kang et al. 2019; Wang et al., 2019). Furthermore, d-excess can effectively  
 292 represent the moisture source properties. The mean d-excess of basin river water during the wet  
 293 season (11.45‰, Table S1) was greater than 10‰, associated with the characteristics of an alpine  
 294 arid continental climate and a moisture source devoid of monsoon influences. Higher d-excess  
 295 values are attributed to westerlies moisture and recycled moisture that is boosted by inland surface  
 296 evaporation. In contrast, the hinterland of the Tibetan Plateau, south of the Tanggula Mountains,  
 297 which was subject to significant influences from the Indian monsoon circulation, had summer  
 298 precipitation and river water d-excess values that ranged from 5‰ to 9‰ with a mean value of 7‰  
 299 (Tian et al., 2001). The stark contrasts in the d-excess values between the two regions further  
 300 support the above inference about the moisture sources of the Qaidam Basin.



301  
 302 **Figure 6.** Tropospheric water vapor flux from June to September 2019 to 2021 (below 500 hPa, unit:  $\text{kg m}^{-1}\text{s}^{-1}$ ).

303 5.1.2 Isotopic records of surface water to precipitation

304 Owing to the sparse precipitation in the alpine arid region and its concentration in summer  
 305 (June to September), surface water isotopic records may mimic local precipitation characteristics  
 306 during the wet season. On a seasonal basis, the positive correlations between isotopic variations in  
 307 surface water (Figure 3) and those in precipitation are extremely strong across most of the basin  
 308 and its surrounding areas (Liu et al., 2009; Zhao et al., 2011; Juan et al., 2020; Wu et al., 2022). In  
 309 particular, the  $\delta^{18}\text{O}$  values in the mountainous areas of each watershed are higher during wet season

310 compared to the dry season, reflecting the input of precipitation with heavy isotopic signatures to  
311 the river. Moreover, the mean  $\delta^{18}\text{O}$  and  $\delta\text{D}$  values are higher in watersheds (such as Qaidam and  
312 Bayin Rivers) during wet season, with correspondingly excessive rainfall (Figure S1). From this,  
313 river water isotopes of each watershed in the basin are primarily impacted by summer precipitation  
314 during the wet season could be inferred. This is mostly because during the rainy season, relatively  
315 intensive rainfall events can create surface runoff and increase river flows rapidly recharge the river.

### 316 5.1.3 Climate impact on isotopic spatial and temporal variation

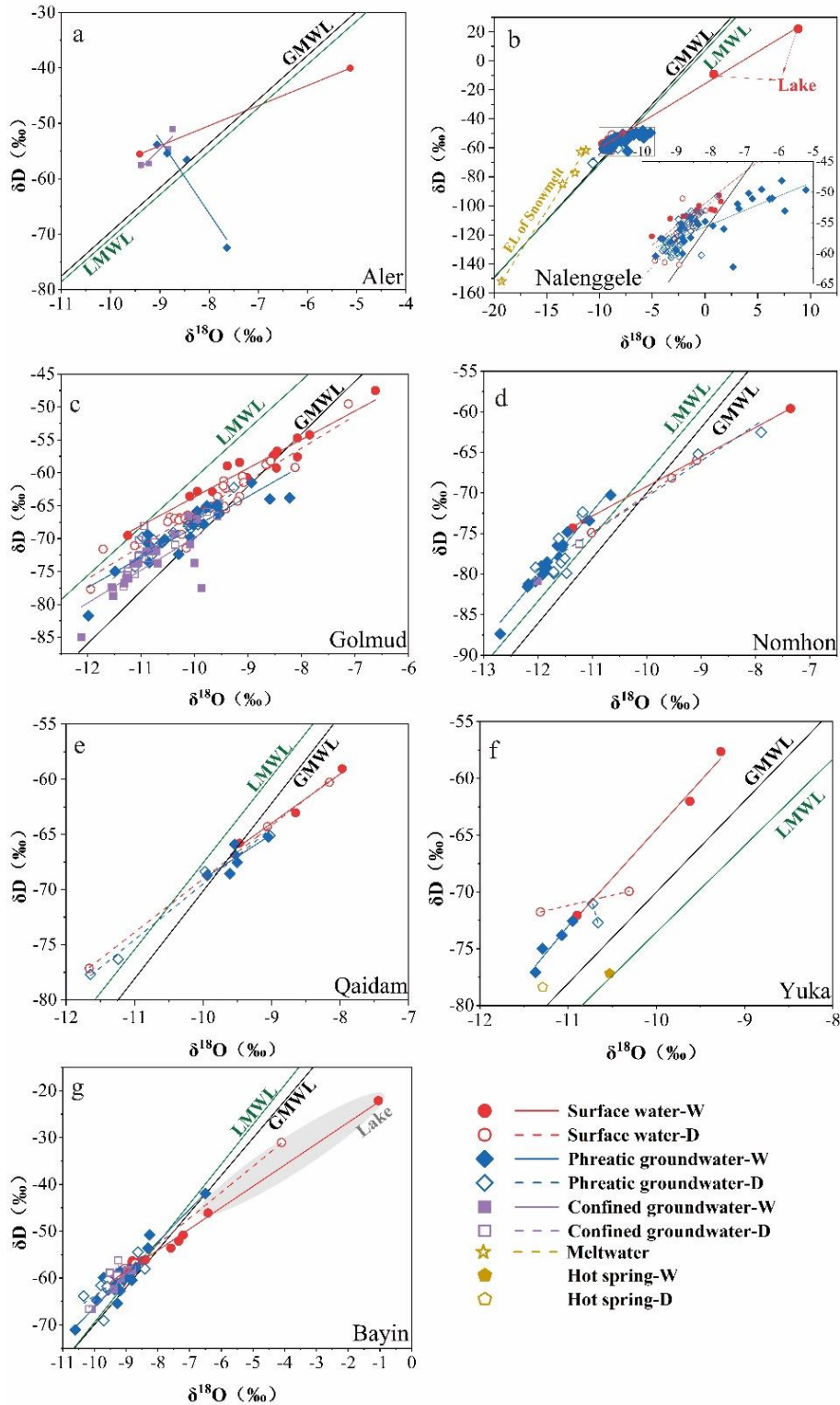
317 The spatial variation of surface water isotopes of the Eastern Kunlun Mountains water system  
318 (Figure 3) reflects the variation of precipitation isotopes which are strongly influenced by  
319 westerlies moisture transport. Heavy isotopes are preferentially separated in raindrops  
320 condensation along the westerlies trajectory, and long distance moisture advection leads to heavy  
321 isotope depleted precipitation due to rainout (Wang et al., 2016; Yang and Wang, 2020).  
322 Meanwhile, the isotope variations in the two watersheds in the Qilian Mountains are opposite to  
323 those in the Eastern Kunlun Mountains. Comparing the meteorological parameters of Delingha  
324 and Da Qaidam (refer to Figure S1 for specific location) from 2010 to 2020, the mean annual  
325 precipitation of Delingha (276.36 mm) was 2.41 times higher than that of Da Qaidam (114.79 mm),  
326 and the mean annual temperature of Delingha (5.23 °C) was 1.58 °C higher than that of Da Qaidam  
327 (3.65 °C). Precipitation in the Bayin River has increased by up to 25.09 mm per decade since 1961  
328 (Figure S1). The seasonal  $\delta^{18}\text{O}$  variation in the Bayin River is roughly 1.79 times that of the Yuka  
329 River, due to the marked increase in precipitation in Delingha. Under similar conditions of  
330 ice/snow meltwater recharge, the mean  $\delta^{18}\text{O}$  and  $\delta\text{D}$  values of the Bayin River are higher than  
331 1.52‰ and 7.3‰, respectively, relative to that of the Yuka River, which can be attributed to a  
332 greater proportional contribution of precipitation with heavy isotopic signatures. As a result, the  
333 change in river water isotopes in the Qilian Mountains can be attributed to the differences in  
334 temperature and precipitation regimes, as well as the extents of warming and humidification  
335 between the watersheds.

336 Given the spatial and temporal variations of surface water  $\delta^{18}\text{O}$ - $\delta\text{D}$  (Figure 3), samples from  
337 different water bodies within each watershed were incorporated into the  $\delta^{18}\text{O}$ - $\delta\text{D}$  plot (Figure 7).  
338 The considerable differences in the dual-isotopic spectrum imply that seasonal variations in  
339 surface water isotopes in each watershed may be attributed to variability in the contribution ratios

340 of precipitation, ice/snow meltwater, and groundwater throughout both the wet and dry seasons.  
341 Hence, Equation 1 of the MixSIAR model was employed to estimate the contribution of each  
342 potential recharge endmember to river water (Table 1). The findings reveal that groundwater  
343 discharge in mountainous areas maintains the base flow in each watershed during dry season, with  
344 groundwater contribution up to 97% of the total flow. Various proportions of precipitation,  
345 ice/snow meltwater and groundwater ~~recharge-feed~~ the river water during the wet season. For  
346 example, in the area with the greatest annual precipitation, the contribution of summer  
347 precipitation to the Bayin River during the wet season may reach 84%. Thus, variability in the  
348 proportional contributions of each recharge endmember during wet and dry seasons are the main  
349 factors responsible for the seasonal variations in surface water isotopes in each watershed.

350 In summary, the spatial and seasonal variations of surface water stable isotopes are caused by  
351 the interaction of regional warming and humidification trends, the intensity of midlatitude  
352 westerlies moisture transport, and local hydrometeorological conditions.





353

354 **Figure 7.**  $\delta^{18}\text{O}$ - $\delta\text{D}$  plots in different water bodies in each watershed of the Qaidam Basin during dry and wet  
 355 seasons. W and D represent wet and dry seasons, respectively. Data source of LMWLs: a and b: Xu et al., 2017;  
 356 c: this study; d and e: Xiao et al., 2017; f: Zhu et al., 2015; g: Tian et al., 2001.

357 **Table 1.** Contribution ratios of endmembers to river water during the wet and dry seasons based on  $\delta^{18}\text{O}$  and  
 358  $d$ -excess (Unit: %; W and D represent wet and dry seasons, respectively).

|             | Endmember | Groundwater | Meltwater | Tributary | Precipitation |
|-------------|-----------|-------------|-----------|-----------|---------------|
| Nalengele-W | Mean      | 0.41        |           | 0.47      | 0.12          |
|             | Max       | 0.60        |           | 0.74      | 0.13          |
|             | Min       | 0.18        |           | 0.27      | 0.08          |
|             | SD        | 0.12        |           | 0.13      | 0.02          |
| Nalengele-D | Mean      | 0.90        | 0.10      |           |               |
|             | Max       | 0.97        | 0.27      |           |               |
|             | Min       | 0.73        | 0.03      |           |               |
|             | SD        | 0.07        | 0.07      |           |               |
| Golmud-W    | Mean      | 0.31        | 0.34      | 0.25      | 0.10          |
|             | Max       | 0.36        | 0.39      | 0.32      | 0.12          |
|             | Min       | 0.28        | 0.29      | 0.20      | 0.08          |
|             | SD        | 0.03        | 0.04      | 0.05      | 0.01          |
| Golmud-D    | Mean      | 0.32        | 0.25      | 0.42      |               |
|             | Max       | 0.46        | 0.45      | 0.70      |               |
|             | Min       | 0.19        | 0.11      | 0.21      |               |
|             | SD        | 0.09        | 0.10      | 0.17      |               |
| Yuka-W      | Mean      | 0.62        | 0.23      |           | 0.15          |
|             | Max       | 0.76        | 0.29      |           | 0.18          |
|             | Min       | 0.55        | 0.15      |           | 0.10          |
|             | SD        | 0.10        | 0.06      |           | 0.04          |
| Bayin-W     | Mean      | 0.26        | 0.04      | 0.25      | 0.45          |
|             | Max       | 0.35        | 0.05      | 0.43      | 0.84          |
|             | Min       | 0.08        | 0.02      | 0.06      | 0.23          |
|             | SD        | 0.08        | 0.01      | 0.11      | 0.19          |

359 5.2 Multi-sources of groundwater recharge and circulation mechanism

360 Seasonal variations in groundwater aquifer H-O isotopes in each watershed suggest that their  
 361 recharge sources, forms, and rates fluctuate. The  $\delta^{18}\text{O}$ - $\delta\text{D}$  correlations of different seasons and  
 362 types of water samples can be used to deduce the groundwater source compositions and recharge  
 363 patterns. According to the seasonal variations in groundwater  $\delta^{18}\text{O}$ - $\delta\text{D}$  in each watershed (Figure  
 364 4) and the dual-isotopic spectrum of different water bodies within the watershed (Figure 7), the  
 365 Qaidam Basin groundwater systems can be divided into three recharge types: modern precipitation  
 366 and glacier snow melt water dominated recharge and fossil water as well.

### 367 5.2.1 Precipitation dominated recharge

368 In the Nalenggele River, which is situated in the southwestern basin, and the Qaidam and  
369 Bayin Rivers in the eastern basin, groundwater  $\delta^{18}\text{O}$  and  $\delta\text{D}$  values are markedly positive in wet  
370 season and negative in dry season (Figure 54). The groundwater isotope data in the majority of the  
371 wet season clusters near the LMWL and GMWL compared to that during the dry season (Figures  
372 7b, 7e, and 7g), indicating the isotopic signatures are similar to the river water and summer  
373 precipitation in the same period (Table S1; Zhu et al., 2015), with different trends in evaporation.  
374 These results suggest precipitation recharges groundwater during the wet season. The significant  
375 seasonal variations of H-O isotopes show that the aquifers in the eastern and southwestern Qaidam  
376 Basin have relatively rapid groundwater circulation and seasonal recharge. There is an abundance  
377 and notable rise in precipitation in the eastern basin (Figure S1). An interesting finding was that  
378 increased precipitation has directly caused a rise of 5 m in water level and an area expansion of  
379 1.59 times in a lake near the headwaters of the Nalenggele River in the southwestern basin from  
380 1995 to 2015 (Chen et al., 2019). The abundant Precipitation observed in the eastern basin  
381 headwater may also be a potential source for the rapid seasonal groundwater recharge associated  
382 with rapid warming and humidification. Furthermore, the tectonic conditions of the recharge area  
383 are believed to enhance seasonal groundwater recharge. The three watersheds coincide with  
384 collision zones of intensive neotectonic movement, where a considerable number of deep faults  
385 and other volcanic channels have developed within recharge areas (Figure 2; Tan et al., 2021). It  
386 can be concluded that favorable hydrological and tectonic conditions facilitate the formation of  
387 directly rapid groundwater recharge of precipitation and meltwater through bedrock fissures at  
388 high altitudes under large hydraulic heads ( $>1000$  m), resulting in significant seasonal variations  
389 in the groundwater H-O isotopes in these regions.

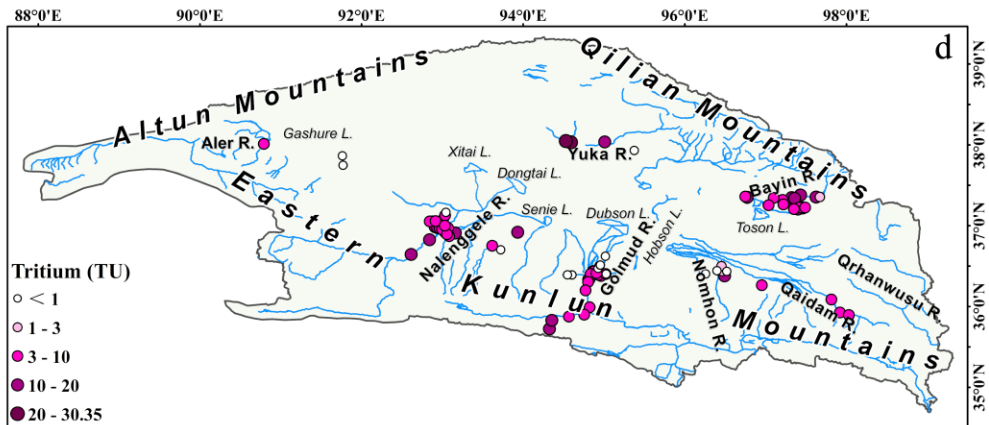
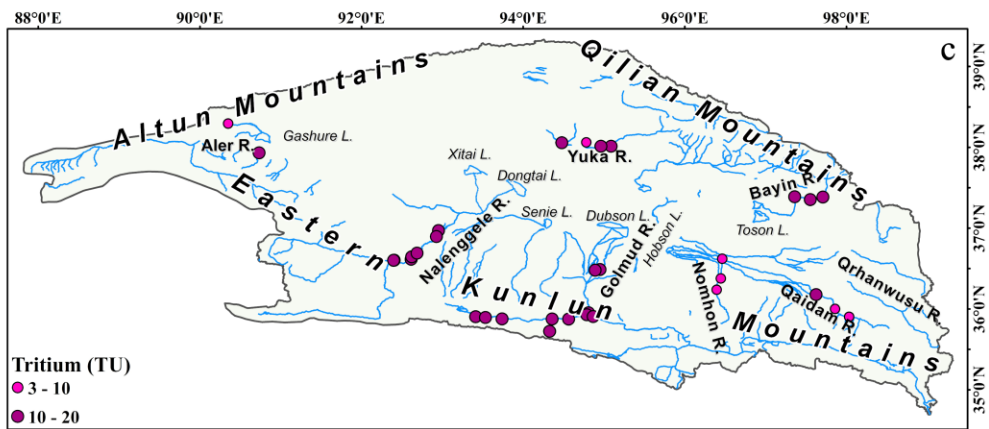
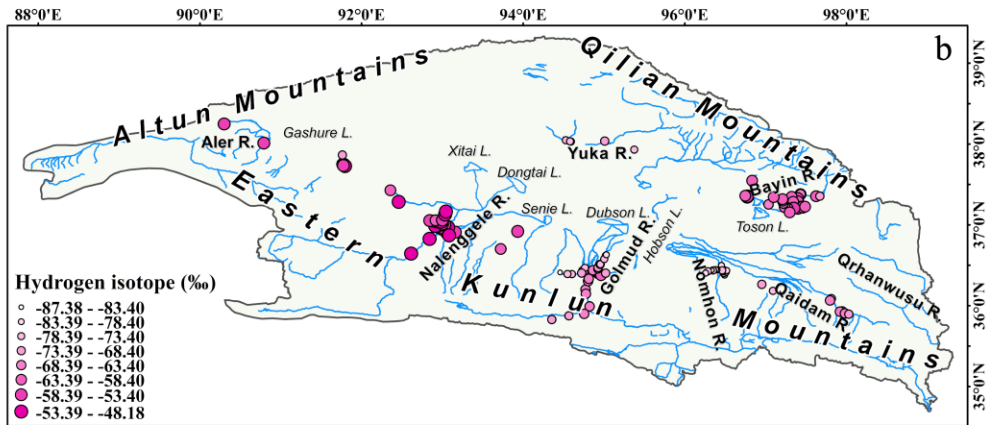
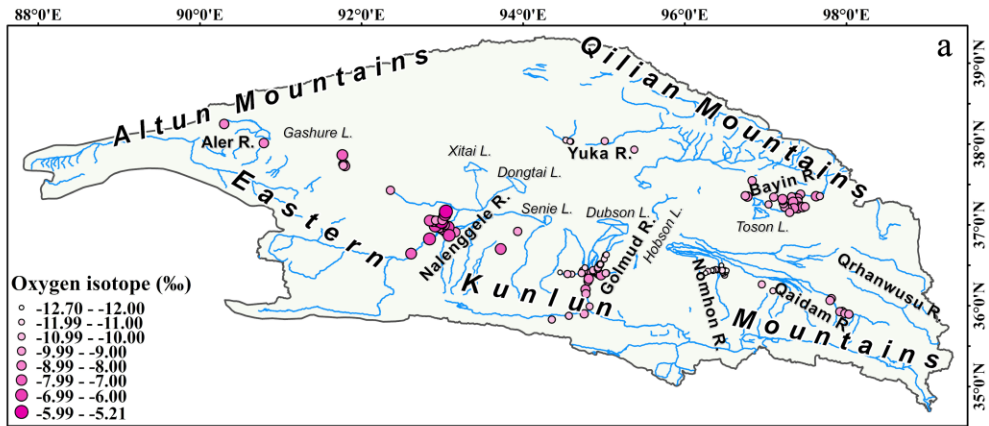
### 390 5.2.2 Glacier snow melt water dominated recharge

391 In the Nomhon and Yuka Rivers, located in the middle region of the basin, groundwater H-O  
392 isotopes are more depleted in the wet season than in the dry season (Table S1; Figure 4). Most of  
393 the  $\delta^{18}\text{O}$ – $\delta\text{D}$  data for the groundwater samples in these two watersheds are observed in the lower  
394 left of the LMWL and GMWL (Figures 7d and 7f), and these values are more negative relative to  
395 river water, with characteristics parallel to those measured in snowmelt water obtained from the  
396 high-altitude Eastern Kunlun Mountain (Figure 5; Yang et al., 2016). This shows that the

397 groundwater recharged by ice/snow meltwater is more isotopically depleted during both the wet  
398 and dry seasons, despite the fact that precipitation contributes less to the aquifer. Similarly, non-  
399 monsoonal meltwater control of hydrological processes in monsoonal groundwater systems has  
400 also been observed on the eastern margin of the Tibetan Plateau (Kong et al., 2019). The isotope  
401 signals suggested that isotopically depleted ice/snow meltwater in the source region was released  
402 due to elevated summer temperatures, and ~~was~~ further depleted ~~in~~ the groundwater after mixing  
403 with groundwater recharged by seasonal meltwater. Furthermore, due to the scarce precipitation  
404 in these two watersheds (61.39 and 121.78 mm, respectively, Figure S1), and that even fewer  
405 precipitation events occurred in 2020, the seasonal direct recharge to the aquifer from the limited  
406 precipitation was negligible in this extremely arid climate.

### 407 5.2.3 Fossil water dominated recharge

408 In the Golmud River, the mean  $\delta^{18}\text{O}$  value is 0.33‰ higher during the wet season than during  
409 the dry season, with insignificant seasonal changes, indicating a limited share of seasonal  
410 groundwater recharge and a slow renewal rate. The groundwater H-O isotope data lay mainly  
411 between the LMWL and GMWL (Figure 7c), implying that the predominant recharge source is the  
412 combination of different periods atmospheric precipitation (Beyerle et al., 1998). Furthermore, the  
413 groundwater  $\delta^{18}\text{O}$  and  $\delta\text{D}$  values exhibit a gradually ~~decreased~~-decreasing trend along the flow  
414 path (Figures 8a and 8b). For this watershed, a prominent feature is the sizeable storage of confined  
415 groundwater, which is constantly discharging at the front edge of the alluvial fan. Confined  
416 groundwater  $\delta^{18}\text{O}$  and  $\delta\text{D}$  values are more negative than those of phreatic groundwater, and the  
417 mean  $\delta^{18}\text{O}$  values are similar during the wet and dry seasons, with minor seasonal variation (Table  
418 S1). We hypothesize that phreatic groundwater is recharged primarily by ice/snow meltwater,  
419 while confined groundwater is slowly and stably recharged and may be sustained by precipitation  
420 with low  $\delta^{18}\text{O}$  and  $\delta\text{D}$  values or fossil water formed during relatively cold climate periods (Xiao  
421 et al., 2018). This scenario is in fact observed in deep confined groundwater in many areas in the  
422 world (Ma et al., 2009; Jasechko et al., 2017).



424 **Figure 8.** Spatial distribution of  $\delta^{18}\text{O}$  (a) and  $\delta\text{D}$  (b) in groundwater and tritium concentrations in surface water  
425 (c) and groundwater (d) during the wet season.

#### 426 5.2.4 Mechanism governing water cycle in alpine mountain-basin system

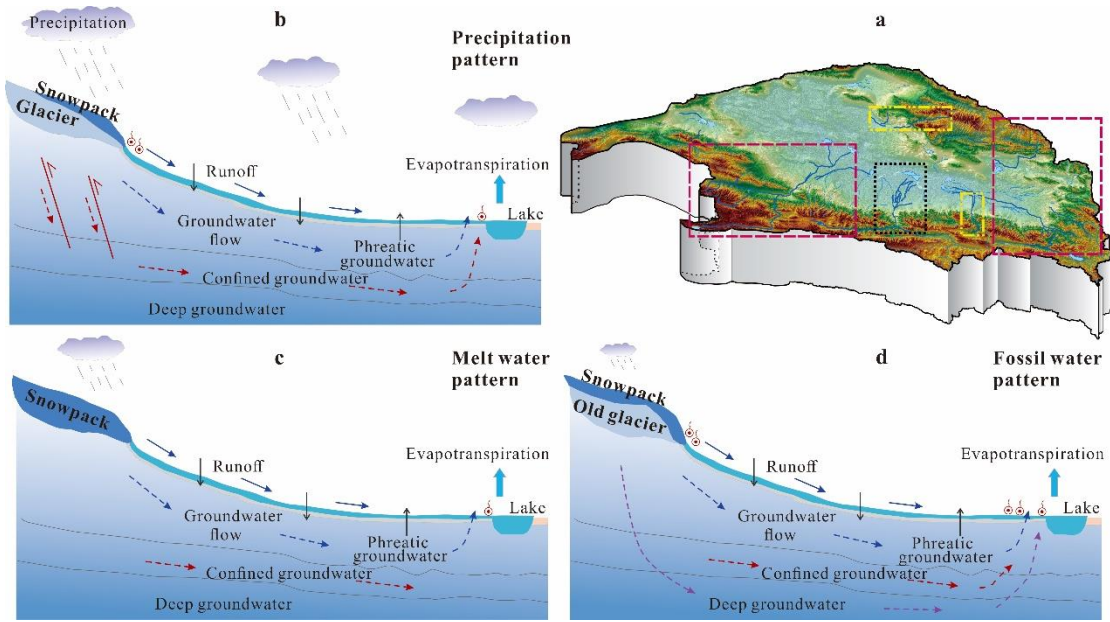
427 Radioactive  $^3\text{H}$ , tritium, with a half-life of 12.32 years, can be used to estimate the migration  
428 time of younger water. Particularly in mixed water bodies consisting of younger water and fossil  
429 water,  $^3\text{H}$  can be used to effectively characterize groundwater age and renewal rate (Stewart et al.,  
430 2017; Xiao et al., 2018; Chatterjee et al., 2019; Shi et al., 2021). In accordance with the significant  
431 differences in  $\delta^{18}\text{O}$ - $\delta\text{D}$  of the various water bodies in each watershed (Figures 7, 8a, and 8b), the  
432 scale of the groundwater recharge in the Qaidam Basin is further constrained with  $^3\text{H}$  (Figures 8c  
433 and 8d). The spatial pattern of  $^3\text{H}$  reveals that groundwater recharge rates varied significantly at  
434 both intra- and inter-watershed scales (Figures 8c and 8d). Thus, the groundwater system is  
435 dominated by both regional and local recharge.

436 At the watershed scale, the  $^3\text{H}$  concentration of phreatic groundwater is significantly higher  
437 in alluvial fan areas along the river channel and mountain pass (Table S1; Figures 8c and 8d), and  
438 approximates that of the river water. This suggests that there is a close hydraulic connection  
439 between surface water and groundwater, and that the aquifer also receives river water through  
440 vertical infiltration and lateral recharge. This portion of groundwater is therefore mostly seasonal,  
441 younger, and has a rather rapid renewal rate.  $^3\text{H}$  concentrations in the periphery of phreatic and  
442 confined groundwater are typically less than 3 TU, indicating that  $^3\text{H}$  is dead in comparison to that  
443 near the river channel. These findings suggest that these aquifers are mostly recharged by lateral  
444 flow, consisting primarily of sub-modern water (>60 years) or fossil water, with limited mixing of  
445 modern precipitation and seasonal meltwater, and a slow renewal rate. This is especially evident  
446 in Golmud and Nomhon Rivers (Liu et al., 2014; Cui et al., 2015; Xiao et al., 2017, 2018),  
447 highlighting the importance of fossil water content in recharging the aquifer in extremely arid  
448 regions.

449 At the basin scale,  $^3\text{H}$  data is consistent with seasonal variations in stable H-O isotopes.  
450 Seasonal variations in  $\delta^{18}\text{O}$  and  $\delta\text{D}$  values correspond to higher average  $^3\text{H}$  concentration in  
451 phreatic groundwater systems in the eastern and southwestern basin, revealing that seasonal  
452 groundwater recharge is more significant, and that groundwater age is overall younger (<60 years).  
453 Based on river seepage, modern meltwater and precipitation may potentially infiltrate through

454 preferential flow paths, such as fault zones developed on a large scale in the recharge area, resulting  
455 in rapid aquifer recharge (Figure 9b; Tan et al., 2021). The contrary was observed in the phreatic  
456 groundwater systems of the western Qilian Mountains and middle Eastern Kunlun Mountains,  
457 where the depletion in heavy isotopes during wet season, accompanied by low  $^3\text{H}$  concentrations,  
458 meant these aquifers were primarily recharged by seasonal ice/snow meltwater. In contrast, the  
459 groundwater renewal rate was relatively slow, owing to ~~less-smaller~~ and ~~more-steady~~steadier  
460 meltwater recharge (Figure 9c).

461 In confined groundwater, heavy H-O isotope depletion is greatest, with most samples having  
462 very low  $^3\text{H}$  concentrations ( $<3$  TU), indicating a very slow recharge rate. Furthermore, most of  
463 the confined groundwater was over 100 years old and consisted mainly of submodern groundwater  
464 or fossil water (Xiao et al., 2018). In the Golmud River, the confined groundwater in the discharge  
465 zone continued to discharge after nearly a half century of extraction, and the pressure heads did  
466 not decrease, implying that modern precipitation or ice/snow meltwater may recharge deep  
467 confined groundwater. Some confined groundwaters possess discernible seasonal isotopic effects,  
468 and the existence of a certain proportion of ongoing recharge, even on a seasonal scale, cannot be  
469 excluded. Large karst springs have also developed in the mountainous areas of Golmud River.  
470 Well-formed karst caves and fissures provide conduits for direct precipitation or meltwater  
471 infiltration. With deep circulation, precipitation and meltwater generate regional subsurface flow  
472 that recharges the confined groundwater in the overflow zone in the long term, allowing continuous  
473 flow under a large hydraulic head (about 1,000 m) (Figure 9d). Moreover, the H-O isotopic signals  
474 of confined groundwater in part of the alluvial fan front in the Golmud and Bayin Rivers are largely  
475 similar with those of the nearby phreatic groundwater, with  $^3\text{H}$  concentrations close to 10 TU.  
476 These findings also suggest that confined groundwater recharge may have occurred through  
477 aquitard or by leakage recharge in nearby skylights.



478

479 **Figure 9.** Schematic diagram of the Qaidam Basin water cycle model (b represents the purple dashed box; c  
 480 represents the yellow dashed box; and d represents the black dashed box).

481 5.3 Isotope hydrology responses to climate change and indication of water cycle trends

482 The Qaidam Basin has experienced rapid warming at a rate more than twice the global  
 483 average since the 1980s (Wang et al., 2014; Kuang and Jiao, 2016; Yao et al., 2022). Since 1961,  
 484 the 10- and 30-year mean temperature and precipitation changes and rising rates at eight  
 485 meteorological stations in the basin have demonstrated that the current warming and  
 486 humidification trends in this basin, northeastern Tibetan Plateau, are continuously strengthening  
 487 (Figure 10). Changes in surface water and groundwater isotopes in the Qaidam Basin reflect  
 488 different sensitivities to climate change at both seasonal and multi-year scales. Previously, it was  
 489 assumed that the isotopic composition of the surface water and groundwater systems did not vary  
 490 with time, at least on interannual intervals, and was rather stable (Boutt et al., 2019). However,  
 491 isotopic measurements variability in water bodies over the past 40 years suggests that there is a  
 492 range variable degree of interannual variability in surface water and groundwater isotopes, with  
 493 interannual variability in mean  $\delta^{18}\text{O}$  values greater than 3‰ (Figure 11). The spatial and temporal  
 494 variability of isotopic signals can be ascribed to differences in the extent of warming and  
 495 humidification across the basins. Wang et al. (2014) highlighted that while the Qaidam Basin has  
 496 experienced rapid warming over the past 50 years, warming and humidification have been  
 497 markedly asynchronous in different regions, with rates of temperature increase ranging from 0.31



498 to 0.89 °C per decade and the rates of rainfall increase from 1.77 to 25.09 mm per decade (Figure  
499 S1). It is noteworthy that surface water is more responsive to precipitation, whereas groundwater  
500 is more sensitive to temperature (Figure 12). This phenomenon suggests that increased  
501 precipitation may influence the water cycle by promoting slope runoff and groundwater infiltration  
502 in mountainous areas, and the warming will cause the solid water ablation at higher elevations,  
503 thereby accelerating groundwater recharge to aquifers through bedrock fissures. In addition,  
504 elegant remote sensing monitoring findings suggested that the increase in terrestrial water storage  
505 in the Qaidam Basin was strongly correlated with increased precipitation and glacier meltwater  
506 recharge (Song et al., 2014; Jiao et al., 2015; Xiang et al., 2016; Wei et al., 2021; Zou et al., 2022),  
507 which fully supported the isotope-based conjecture. Furthermore, a recent study found that the  
508 accelerated conversion of ice and snow into liquid water on the Tibetan Plateau has led to an  
509 imbalance in the “Asia Water Tower”, with the Qaidam Basin being one of the key regions where  
510 liquid water has grown (Yao et al., 2022). The isotopes, remote sensing and hydrometeorology  
511 data are consistent with the observation that the Qaidam Basin is the most rapid and substantial  
512 warming region in the Tibetan Plateau. Global warming affects the basin by redistributing  
513 precipitation and melting ice and snow in high elevations, resulting in groundwater storage  
514 increases and lakes expansions. The trend of increasing water storage in the Qaidam Basin is likely  
515 to continue in the 21st century. The highly coupled results of different observation methods further  
516 emphasize the sensitivity and potential of water isotopes in tracing water cycles and climate change.

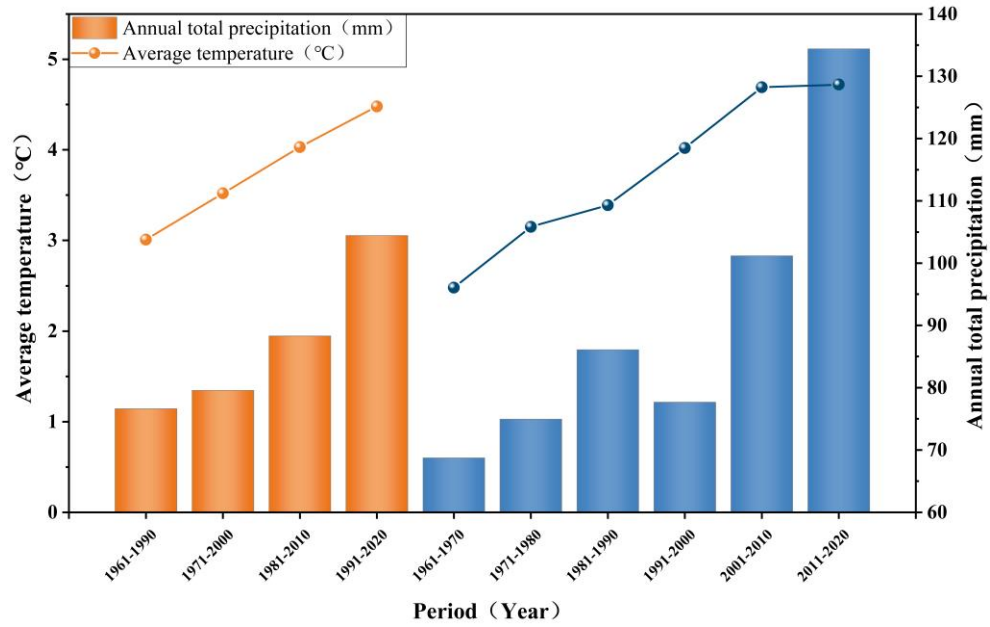
517 Under the influence of climate change and the intensive cryosphere retreat, runoff has  
518 changed dramatically on the Tibetan Plateau, with significant effects on the spatial and temporal  
519 water resources distribution (Wang et al., 2021). The rapid changes in water resources in the  
520 Qaidam Basin are likely because:

521 1) The surface water and groundwater resources will increase significantly in the short term  
522 (in recent decades) due to continued rapid warming and wetting. For example, water storage  
523 in the Bayin and Qaidam Rivers in the eastern basin is likely to continue to increase with a  
524 high renewal capacity in the long term under the influence of sustained climate change and  
525 the abundant and significantly increasing precipitation. This phenomenon has been verified  
526 in many regions of the Tibetan Plateau as well as some alpine watersheds in high-latitude  
527 Switzerland (Xiang et al., 2016; Malard et al., 2016; Shi et al., 2021).

528 2) The decadal scale climatic oscillation suggests that the massive shrinking cryosphere may  
529 not sustain surface water and groundwater recharge in the basin (Wang et al., 2023). It is  
530 expected that water resources in the southwestern basin (e.g., Nalenggele River) may  
531 continue to increase for a certain period followed by a large-scale decrease under future  
532 climate change scenarios. This is a general trend that has occurred in the Tibetan Plateau as  
533 well as regions around the world with large-scale glacial coverage area in alpine watersheds.  
534 Glaciers in the southwestern basin are reported to be losing mass regularly ( $-0.2$  to  $-0.5$   
535 m/a), a trend that has increased substantially from 2018 to 2020, notably at the headwaters  
536 of Nalenggele River, where glacier elevation has been reduced by 5.42 m since 2000 (Shen  
537 et al., 2022). However, completing the hydrologic budget will remain a challenge given  
538 strong decoupling between rapid melting of ice and snow caused by warming versus scarce  
539 precipitation in the southwestern basin, even if precipitation continuously increases in the  
540 future.

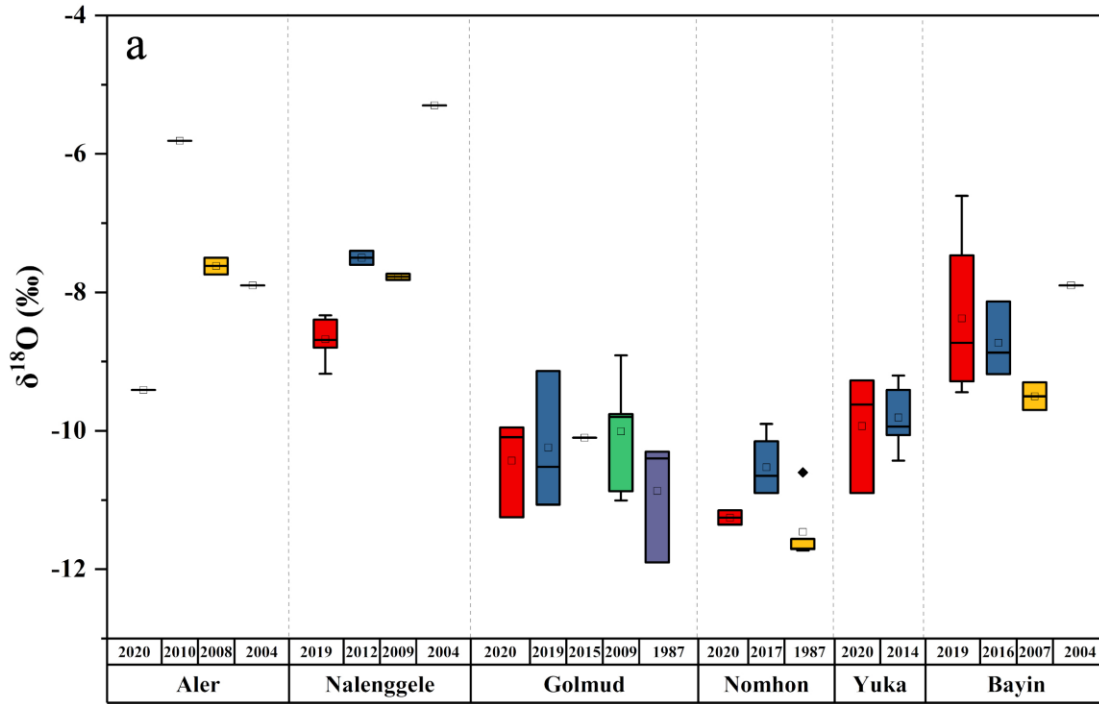
541 3) In the middle basin (Nomhon, Golmud, and Yuka Rivers), there is long-term large-scale  
542 groundwater mining during the agriculture and industry development, accompanied by  
543 strong local evaporation. The sparse precipitation in the source area led to a melt  
544 dependence, although the surface water and groundwater recharge here are relatively stable.

545 4) Future groundwater level dropping seems to be inevitable in the basin with glacier retreat  
546 and reducing of melt water in the mountainous source area. Monitoring data from five  
547 shallow groundwater boreholes along the alluvial fan belt of the Golmud River shows that  
548 groundwater levels have fluctuated since 2011, declining by an average of  $-1.18$  m/a  
549 (Figure S2). Therefore, whether the enhanced water resource renewal capacity and water  
550 storage in the Qaidam Basin can stay stable in the future is a scientific issue worth  
551 considering.

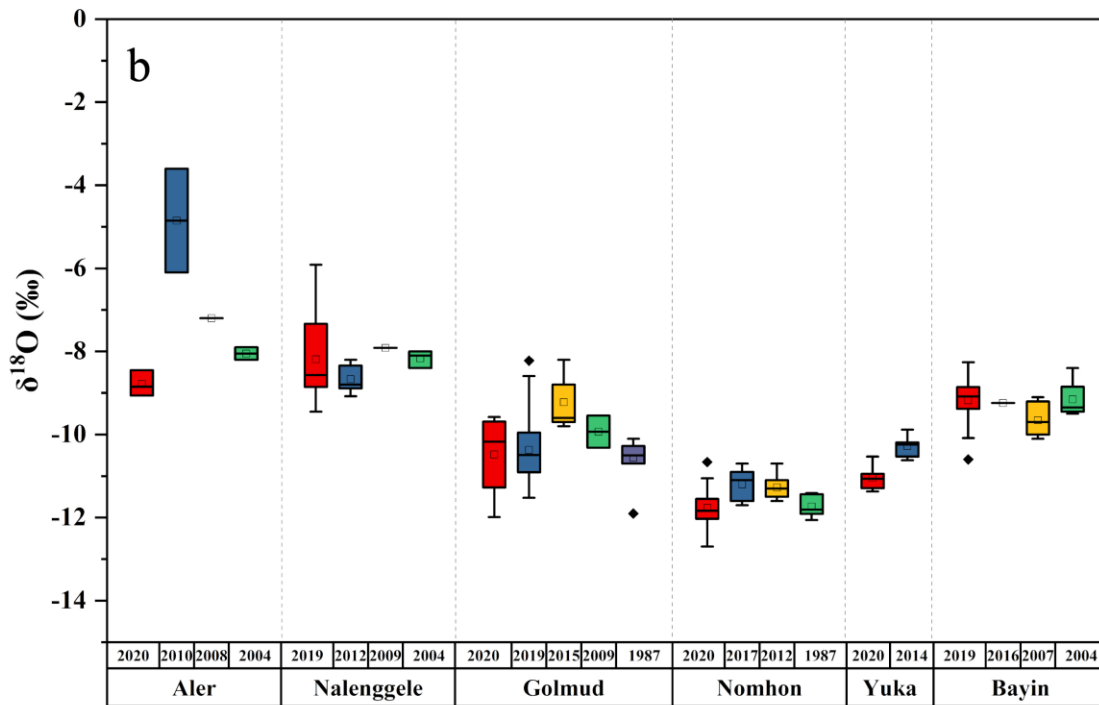


552

553 **Figure 10.** Average temperature and precipitation in the Qaidam Basin every 30 years and 10 years from 1961  
 554 to 2020.



Year/Watershed



Year/Watershed

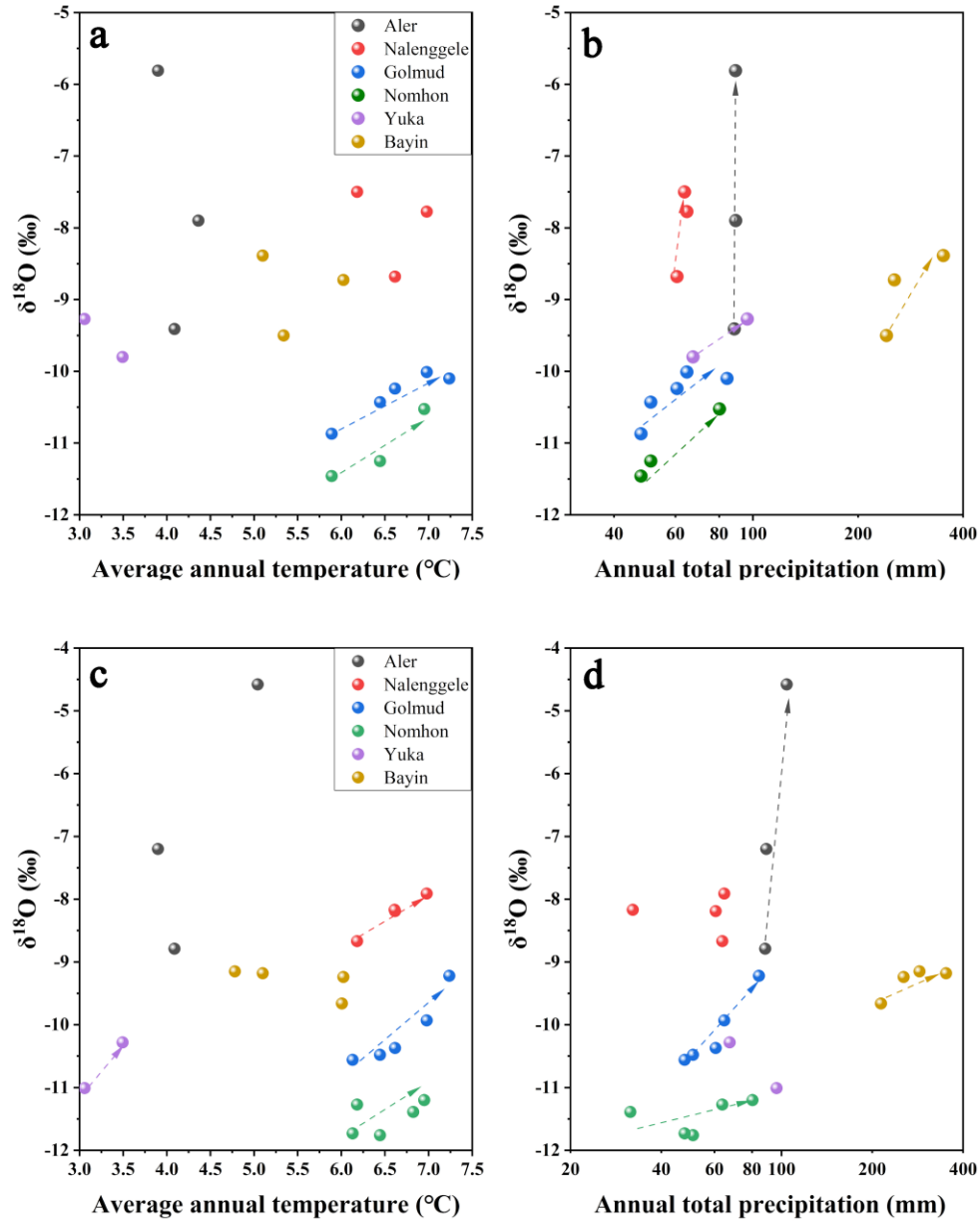
555

556 **Figure 11.** Interannual variations in the river water (a) and groundwater (b)  $\delta^{18}\text{O}$  in the Qaidam Basin. Date

557 source: Aler: 2004, Wang et al., 2008; 2008, Tan et al., 2009; 2010, Ye et al., 2015. Nalenggele: 2004,

558 Wang et al., 2008; 2009, Tan et al., 2012; 2012, Xu et al., 2017. Golmud: 1987, Wang et al., 2008; 2009,

559 Tan et al., 2012; 2015, Xiao et al., 2018. Nomhon: 1987, Wang et al., 2008; 2012, Cui et al., 2015; 2017,  
 560 Zhao et al., 2018. Yuka: 2014, Zhu, 2015. Bayin: 2004, Wang et al., 2008; 2007, He et al., 2016; 2016,  
 561 Wen et al., 2018.



562

563 **Figure 12.** Surface water  $\delta^{18}\text{O}$  and temperature (a) and precipitation (b); Groundwater  $\delta^{18}\text{O}$  and temperature (c)  
 564 and precipitation (d) in the Qaidam Basin. The light lines indicate  $\delta^{18}\text{O}$  change with temperature and  
 565 precipitation.

## 566 6. Conclusion

567 The spatial and temporal variations of  $\delta^{18}\text{O}$  and  $\delta\text{D}$  in surface water and groundwater of the  
568 Qaidam Basin reflect their dynamic hydrological responses to climate change, water sources, and  
569 local temperature and precipitation regimes, especially precipitation, at interannual and seasonal  
570 scales.

571 (1) The mean values of surface water  $\delta^{18}\text{O}$  and  $\delta\text{D}$  in the Eastern Kunlun Mountains gradually  
572 decrease eastward, whereas the opposite is true for the Qilian Mountains river system, reflecting  
573 the intensity of westerlies moisture transport and the influence of local climatic conditions,  
574 respectively. Surface water is enriched in heavy H-O isotopes during wet season and is relatively  
575 depleted during dry season. ~~The River~~ base flow is maintained by groundwater ~~recharge-discharge~~  
576 during dry season, ~~and rivers receive while receiving~~ varying proportions of groundwater (26%–  
577 62%), ice/snow meltwater (23%–47%) and precipitation (10%–45%) during wet season. The  
578 seasonal isotopic variability is determined by the quantity of precipitation and its gradient in the  
579 basin, with precipitation in the Qilian Mountains contributing more to rivers than in the eastern  
580 Kunlun Mountains.

581 (2) The key factor accelerating groundwater circulation in the Qaidam Basin is the  
582 contribution of precipitation and meltwater produced by climate change. The groundwater systems  
583 located in the collision and convergence zone of several mountain ranges are distinguished by  
584 enriched H-O isotopes during wet season, high  $^3\text{H}$  concentrations, and marked rapid seasonal  
585 recharge. Modern precipitation and meltwater can infiltrate through favorable structural conduits  
586 (e.g., large-scale active fault zones), resulting in rapid groundwater recharge. In contrast, the  
587 groundwater systems in the western Qilian Mountains and the middle Eastern Kunlun Mountains  
588 are depleted in H-O isotopes during wet season and  $^3\text{H}$  concentrations are low, and are primarily  
589 slowly recharged by seasonal ice/snow meltwater, which consisted of modern water and  
590 submodern water (>60 years). The confined groundwater is considerably depleted in H-O isotopes,  
591 and for the most part exhibits imperceptible seasonal changes.  $^3\text{H}$  concentrations are very low, and  
592 recharge is quite slow, dominated by fossil water.

593 (3) Warming climate has exerted a substantial impact on the hydrological processes across  
594 the basin, accelerating ~~the~~ water cycle and ~~raising-increasing~~ water storage ~~uncertainties~~ in the  
595 eastern and southwestern basin through the increased precipitation and melting of glaciers and

596 snow. However, this increasing trend of water resources in the basin seems to be unsustainable.  
597 The southwestern basin could suffer a rapid loss in total water resources in the future as  
598 precipitation increases and solid water ablation in mountainous areas ~~becoming~~becomes severely  
599 out of balance ~~undergone~~due to climatic extreme changes.

#### 600 **Author Contribution**

601 Conceptualization: Yu Zhang, Hongbing Tan; Funding acquisition: Xiyang Zhang;  
602 Investigation: Peixin Cong; Resources: Wenbo Rao; Visualization: Dongping Shi; Writing–  
603 original draft: Yu Zhang; Writing–review & editing: Hongbing Tan.

#### 604 **Acknowledgments**

605 This study was financially supported by the National Natural Science Foundation of China  
606 (U22A20573), the Second Tibetan Plateau Scientific Expedition and Research Program (STEP)  
607 (2022QZKK0202), the Fundamental Research Funds for the Central Universities (B230205010),  
608 and the Postgraduate Research & Practice Innovation Program of Jiangsu Province  
609 (KYCX22\_0666). We thank the editors, Prof. Michael K. Stewart and the other two anonymous  
610 reviewers for providing a list of critical and very valuable comments that helped to improve the  
611 manuscript. We also thank Prof. Beckie, R. D. for writing suggestions and thoughtful reviews with  
612 the final revision. We would like to express our gratitude for all members' help both in the field  
613 observation and geochemical analysis in the laboratory.

#### 614 **Declaration of interests**

615 The authors declare that they have no known competing financial interests or personal  
616 relationships that could have appeared to influence the work reported in this paper.

#### 617 **Data Availability Statement**

618 The complete list of isotopes and their values is available in Table S1 in Supporting  
619 Information. The meteorological data can be obtained on China Meteorological Data Network  
620 (<http://data.cma.cn>). The monthly mean ERA5 reanalysis data ( $0.25^\circ \times 0.25^\circ$ ) can be obtained from  
621 European Centre for Medium-Range Weather Forecasts (ECMWF, <https://www.ecmwf.int/>).

#### 622 **References**

623 Ahmed, M., Chen, Y., ~~& and~~ Khalil, M. M. (2022).: Isotopic Composition of Groundwater  
624 Resources in Arid Environments-. ~~J. Hydrol. Journal of Hydrology~~, ~~609~~, 127773,  
625 ~~https://doi.org/10.1016/j.jhydrol.2022.127773~~, 2022.

626 Bam, E. K, Ireson, A. M, van Der Kamp, G., ~~& and~~ Hendry, J. M. (2020).: Ephemeral ponds: Are  
627 they the dominant source of depression-focused groundwater recharge?-. ~~Water. Resour.~~  
628 ~~Res. Water Resources Research~~, 56(3), e2019WR026640,  
629 ~~https://doi.org/10.1029/2019WR026640~~, 2020.

630 Befus, K. M, Jasechko, S., Luijendijk, E., Gleeson, T., ~~& and~~ Bayani Cardenas, M. (2017).: The  
631 rapid yet uneven turnover of Earth's groundwater-. ~~Geophys. Res. Lett. Geophysical Research~~  
632 ~~Letters~~, 44(11), 5511-5520, ~~https://doi.org/10.1002/2017GL073322~~, 2017.

633 Benettin, P., Rodriguez, N. B., Sprenger, M., Kim, M., Klaus, J., Harman, C. J., ~~Van Der Velde,~~  
634 ~~Y., Hrachowitz, M., Botter, G., McGuire, K. J., Kirchner, J. W., Rinaldo, A., ... & and~~  
635 McDonnell, J. J. (2022).: Transit time estimation in catchments: Recent developments and  
636 future directions-. ~~Water. Resour. Res. Water Resources Research~~, 58(11), e2022WR033096,  
637 ~~https://doi.org/10.1029/2022WR033096~~, 2022.

638 Beyerle, U., Purtschert, R., Aeschbach-Hertig, W., Imboden, D. M., Loosli, H. H., Wieler, R., ~~&~~  
639 ~~and~~ Kipfer, R. (1998).: Climate and groundwater recharge during the last glaciation in an ice-  
640 covered region-. ~~Science~~, 282(5389), 731-734, ~~https://doi.org/10.1126/science.282.5389.731~~,  
641 ~~1998~~.

642 Boutt, D. F., Mabee S. B., ~~and~~ Yu, Q.: Multiyear increase in the stable isotopic composition of  
643 stream water from groundwater recharge due to extreme precipitation{H}. ~~Geophys. Res.~~  
644 ~~Lett. Geophysical Research Letters~~, 2019, 46(10:—), 5323-5330,  
645 ~~https://doi.org/10.1029/2019GL082828~~, 2019.

646 Bowen, G. J., Cai, Z., Fiorella, R. P., ~~& and~~ Putman, A. L. (2019).: Isotopes in the water cycle:  
647 regional-to global-scale patterns and applications-. ~~Annu. Rev. Earth. Pl. Sc. Annual Review~~  
648 ~~of Earth and Planetary Sciences~~, 47(1), 453-479, ~~https://doi.org/10.1146/annurev-earth-~~  
649 ~~053018-060220~~, 2019.

650 Chang, Q., Ma, R., Sun, Z., Zhou, A., Hu, Y., ~~& and~~ Liu, Y. (2018).: Using isotopic and  
651 geochemical tracers to determine the contribution of glacier-snow meltwater to streamflow  
652 in a partly glacierized alpine-gorge catchment in northeastern Qinghai-Tibet Plateau-. ~~J.~~



653 ~~Geophys. Res-Atmos.~~ ~~Journal of Geophysical Research: Atmospheres~~, 123(18), 10-037,  
654 <https://doi.org/10.1029/2018JD028683>, 2018.

655 Chatterjee, S., Gusyev, M. A., Sinha, U. K., Mohokar, H. V., & Dash, A. (2019):  
656 Understanding water circulation with tritium tracer in the Tural-Rajwadi geothermal area,  
657 India. ~~Appl. Geochem.~~ ~~Applied Geochemistry~~, 109, 104373,  
658 <https://doi.org/10.1016/j.apgeochem.2019.104373>, 2019.

659 Chen, C., Zhang, X., Lu, H., Jin, L., Du, Y., & Chen, F. (2021): Increasing summer precipitation  
660 in arid Central Asia linked to the weakening of the East Asian summer monsoon in the recent  
661 decades. ~~Int. J. Climatol.~~ ~~International Journal of Climatology~~, 41(2), 1024-1038,  
662 <https://doi.org/10.1002/joc.6727>, 2021.

663 Chen, J., Wang Y., Zheng, J., & Cao L. (2019): The changes in the water volume of  
664 Ayakekumu Lake based on satellite remote sensing data. ~~Journal of Natural Resources~~, 34(6),  
665 1331- 1344, [10.31497/zrzyxb.20190618](https://doi.org/10.31497/zrzyxb.20190618), 2019 (in Chinese with English abstract).

666 Clark, I. D., & Fritz, P. (2013) (1st ed.): Environmental isotopes in hydrogeology. ~~CRC press~~,  
667 ~~Boca Raton~~, 342 pp., ISBN 9780429069574, 1997.

668 Condon, L. E., Atchley, A. L., & Maxwell, R. M. (2020): Evapotranspiration depletes  
669 groundwater under warming over the contiguous United States. ~~Nat. Commun.~~ ~~Nature~~  
670 ~~communications~~, 11(1), 1-8, <https://doi.org/10.1038/s41467-020-14688-0>, 2020.

671 Craig, H. (1961): Isotopic variations in meteoric waters. ~~Science~~, 133(3465), 1702-1703,  
672 <https://doi.org/10.1126/science.133.3465.170>, 1961.

673 Cui, Y., ~~Li~~ Liu, F., & Hao, Q. (2015): Characteristics of hydrogen and oxygen isotopes and  
674 renewability of groundwater in the Nuomuhong alluvial fan. ~~Hydrogeology & Engineering~~  
675 ~~Geology~~, 42(6), 1-7, <https://doi.org/10.16030/j.cnki.issn.1000-3665.2015.06.01>, 2015 (in  
676 Chinese with English abstract).

677 Dansgaard, W. (1964): Stable isotopes in precipitation. ~~tellus~~, 16(4), 436-468,  
678 <https://doi.org/10.3402/tellusa.v16i4.8993>, 1964.

679 Durack, P. J., Wijffels, S. E., & Matear, R. J. (2012): Ocean salinities reveal strong global  
680 water cycle intensification during 1950 to 2000. ~~Science~~, 336(6080), 455-458,  
681 <https://doi.org/10.1126/science.1212222>, 2012.

682 Haddeland, I., Heinke, J., Biemans, H., Eisner, S., Flörke, M., Hanasaki, N., ~~Konmann, Ma.~~,  
683 ~~Ludwig, F.~~, ~~Masaki, Y.~~, ~~Schewe, J.~~, ~~Stacke, T.~~, ~~Tessler, Z. D.~~, ~~Wada, Y.~~, & ~~Wisser, D.~~

684 ~~(2014):~~ Global water resources affected by human interventions and climate change-. P. Natl.  
685 Acad. Sci. Usa. Proceedings of the National Academy of Sciences, 111(9), 3251-3256,  
686 <https://doi.org/10.1073/pnas.122247511>, 2014.

687 He, Y., Zhao, C., Liu, Z., Wang, H., Liu, W., Yu, Z., ~~Zhao, Y., ... & and~~ Ito, E. ~~(2016):~~ Holocene  
688 climate controls on water isotopic variations on the northeastern Tibetan Plateau-. Chemical  
689 Geology Chem. Geol., 440, 239-247, <https://doi.org/10.1016/j.chemgeo.2016.07.024>, 2016.

690 Hooper, R. P. ~~(2003):~~ Diagnostic tools for mixing models of stream water chemistry-. Water.  
691 Resour. Res. Water Resources Research, 39(3), 1055,  
692 <https://doi.org/10.1029/2002WR001528>, 2003.

693 Hooper, R. P., Christophersen, N., & and Peters, N. E. ~~(1990):~~ Modeling streamwater chemistry  
694 as a mixture of soilwater end-members—An application to the Panola Mountain catchment,  
695 Georgia, USA. J. Hydrol. Journal of Hydrology, 116(1-4), 321-343,  
696 [https://doi.org/10.1016/0022-1694\(90\)90131-G](https://doi.org/10.1016/0022-1694(90)90131-G), 1990.

697 Huntington, T. G. ~~(2006):~~ Evidence for intensification of the global water cycle: review and  
698 synthesis. J. Hydrol. Journal of Hydrology, 319(1-4), 83-95,  
699 <https://doi.org/10.1016/j.jhydrol.2005.07.003>, 2006.

700 Jasechko, S., Birks, S. J., Gleeson, T., Wada, Y., Fawcett, P. J., Sharp, Z. D., ~~McDonnell, J.J., ...~~  
701 ~~& and~~ Welker, J. M. ~~(2014):~~ The pronounced seasonality of global groundwater recharge.  
702 Water. Resour. Res. Water Resources Research, 50(11), 8845-8867,  
703 <https://doi.org/10.1002/2014WR015809>, 2014.

704 Jasechko, S., Perrone, D., Befus, K. M., Bayani Cardenas, M., Ferguson, G., Gleeson, T.,  
705 Luijendijk, E., McDonnell, J. J., Taylor, R. G., Wada, Y., ... & and Kirchner, J. W. ~~(2017):~~  
706 Global aquifers dominated by fossil groundwaters but wells vulnerable to modern  
707 contamination. Nat. Geosci. Nature Geoscience, 10(6), 425-429,  
708 <https://doi.org/10.1038/ngeo2943>, 2017.

709 Jiao, J. J., Zhang, X., Liu, Y., & and Kuang, X. ~~(2015):~~ Increased water storage in the Qaidam  
710 Basin, the North Tibet Plateau from GRACE gravity data-. Plos. One. PloS one, 10(10),  
711 e0141442, <https://doi.org/10.1371/journal.pone.0141442>, 2015.

712 Juan, G., Li, Z., Qi, F., Ruifeng, Y., Tingting, N., Baijuan, Z., Jian, X., Wende, G., Fusen, N.,  
713 Weixuan, N., Anle, Y., and Pengfei, L. :Environmental effect and spatiotemporal pattern of  
714 stable isotopes in precipitation on the transition zone between the Tibetan Plateau and arid

715 [region, Sci. Total. Environ., 749, 141559, https://doi.org/10.1016/j.scitotenv.2020.141559,](https://doi.org/10.1016/j.scitotenv.2020.141559)  
716 [2020.](https://doi.org/10.1016/j.scitotenv.2020.141559)

717 Kang, S., Cong, Z., Wang, X., Zhang, Q., Ji, Z., Zhang, Y., ~~& and~~ Xu, B. (2019): The  
718 transboundary transport of air pollutants and their environmental impacts on Tibetan Plateau,  
719 ~~Chinese. Sci. Bull.Chinese Science Bulletin~~, 64(27), 2876-2884, [https://doi.org/10.1360/TB-](https://doi.org/10.1360/TB-2019-0135)  
720 [2019-0135, 2019.](https://doi.org/10.1360/TB-2019-0135)

721 Ke, L., Song, C., Wang, J., Sheng, Y., Ding, X., Yong, B., ~~Ma, R., Liu, K., Zhan, P., ... & and~~  
722 Luo, S. (2022): Constraining the contribution of glacier mass balance to the Tibetan lake  
723 growth in the early 21st century-, ~~Remote. Sens. Environ.Remote Sensing of Environment~~,  
724 268, 112779, [https://doi.org/10.1016/j.rse.2021.112779, 2022.](https://doi.org/10.1016/j.rse.2021.112779)

725 Kong, Y., Wang, K., Pu, T., ~~& and~~ Shi, X. (2019): Nonmonsoon precipitation dominates  
726 groundwater recharge beneath a monsoon-affected glacier in Tibetan Plateau-, ~~J. Geophys.~~  
727 ~~Res-AtmosJournal of Geophysical Research: Atmospheres~~, 124(20), 10913-10930,  
728 [https://doi.org/10.1029/2019JD030492, 2019.](https://doi.org/10.1029/2019JD030492)

729 Kuang, X., ~~& and~~ Jiao, J. J (2016): Review on climate change on the Tibetan Plateau during the  
730 last half century-, ~~J. Geophys. Res-Atmos.Journal of Geophysical Research: Atmospheres~~,  
731 121(8), 3979-4007, [https://doi.org/10.1002/2015JD024728, 2016.](https://doi.org/10.1002/2015JD024728)

732 Li, L., ~~& and~~ Garzzone, C. N (2017): Spatial distribution and controlling factors of stable isotopes  
733 in meteoric waters on the Tibetan Plateau: Implications for paleoelevation reconstruction-,  
734 ~~Earth. Planet. Sci. Lett.Earth and Planetary Science Letters~~, 460, 302-314,  
735 [https://doi.org/10.1016/j.epsl.2016.11.046, 2017.](https://doi.org/10.1016/j.epsl.2016.11.046)

736 Li, L., Shen, H., Li, H., ~~& and~~ Xiao, J. (2015): Regional differences of climate change in Qaidam  
737 Basin and its contributing factors-, ~~Journal of Natural Resources~~, 30, 641-650, [2015](https://doi.org/10.1016/j.jnr.2015.05.001) (in  
738 Chinese with English abstract).

739 Liu, F., Cui, Y., Zhang, G., Geng, F., ~~& and~~ Liu, J. (2014): Using the 3H and 14C dating methods  
740 to calculate the groundwater age in Nuomuhong, Qaidam Basin-, ~~Geoscience~~, 28 (6), 1322-  
741 1328, [2014](https://doi.org/10.1016/j.geoscience.2014.06.001) (in Chinese with English abstract).

742 Liu, J., Song, X., Sun, X., Yuan, G., Liu, X., ~~& and~~ Wang, S. (2009): Isotopic composition of  
743 precipitation over Arid Northwestern China and its implications for the water vapor origin-,  
744 ~~J. Geogr. Sci.Journal of Geographical Sciences~~, 19(2), 164-174,  
745 [https://doi.org/10.1007/s11442-009-0164-3, 2009.](https://doi.org/10.1007/s11442-009-0164-3)

746 Ma, J., Ding, Z., Edmunds, W. M., Gates, J. B., & Huang, T. (2009): Limits to recharge of  
747 groundwater from Tibetan plateau to the Gobi desert, implications for water management in  
748 the mountain front—, J. Hydrol. Journal of Hydrology, 364(1-2), 128-141,  
749 <https://doi.org/10.1016/j.jhydrol.2008.10.010>, 2009.

750 Malard, A., Sinreich, M., & Jeannin, P. Y. (2016): A novel approach for estimating karst  
751 groundwater recharge in mountainous regions and its application in Switzerland—, Hydrol.  
752 Process. Hydrological Processes, 30(13), 2153-2166, <https://doi.org/10.1002/hyp.10765>,  
753 2016.

754 Masson-Delmotte, V., Zhai, P., Pirani, A., Connors, S. L., Péan, C., Berger, S., Huang, M., Yelekçi,  
755 O., Yu, R., ... & Zhou, B. (2021): Climate change 2021: the physical science basis.  
756 Contribution of working group I to the sixth assessment report of the intergovernmental panel  
757 on climate change, 2, <https://doi.org/10.1017/9781009157896>, 2021.

758 Moran, B. J., Boutt, D. F., & Munk, L. A. (2019): Stable and radioisotope systematics reveal  
759 fossil water as fundamental characteristic of arid orogenic-scale groundwater systems—, Water.  
760 Resour. Res. Water Resources Research, 55(12), 11295-11315,  
761 <https://doi.org/10.1029/2019WR026386>, 2019.

762 Parnell, A. C., Inger, R., Bearhop, S., & Jackson, A. L. (2010): Source partitioning using stable  
763 isotopes: coping with too much variation—, PLoS Plos. One., 5(3), e9672,  
764 <https://doi.org/10.1371/journal.pone.0009672>, 2010.

765 Rodriguez, N. B., Pfister, L., Zehe, E., & Klaus, J. (2021): A comparison of catchment travel  
766 times and storage deduced from deuterium and tritium tracers using StorAge Selection  
767 functions—, Hydrol. Earth. Syst. Sci., 25(1), 401-428, [https://doi.org/10.5194/hess-25-401-](https://doi.org/10.5194/hess-25-401-2021)  
768 [2021](https://doi.org/10.5194/hess-25-401-2021), 2021.

769 Shen, C., Jia, L., & Ren, S. (2022): Inter-and Intra-Annual Glacier Elevation Change in High  
770 Mountain Asia Region Based on ICESat-1&2 Data Using Elevation-Aspect Bin Analysis  
771 Method—, Remote. Sens. basel. Remote Sensing, 14(7), 1630,  
772 <https://doi.org/10.3390/rs14071630>, 2022.

773 Shi, D., Tan, H., Chen, X., Rao, W., & Basang, R. (2021): Uncovering the mechanisms of  
774 seasonal river-groundwater circulation using isotopes and water chemistry in the middle  
775 reaches of the Yarlungzangbo River, Tibet—, J. Hydrol. Journal of Hydrology, 603, 127010,  
776 <https://doi.org/10.1016/j.jhydrol.2021.127010>, 2021.

- 777 Song, C., Huang, B., Richards, K., Ke, L., ~~& and~~ Hien Phan, V. (2014): Accelerated lake  
778 expansion on the Tibetan Plateau in the 2000s: Induced by glacial melting or other  
779 processes? ~~?, Water. Resour. Res.~~ ~~Water Resources Research~~, 50(4), 3170-3186,  
780 <https://doi.org/10.1002/2013WR014724>, 2014.
- 781 Stewart, M. K., Morgenstern, U., Gusyev, M. A., ~~& and~~ Maloszewski, P. (2017): Aggregation  
782 effects on tritium-based mean transit times and young water fractions in spatially  
783 heterogeneous catchments and groundwater systems ~~-, Hydrol. Earth. Syst. Sci.~~ ~~Hydrology~~  
784 ~~and Earth System Sciences~~, 21(9), 4615-4627, <https://doi.org/10.5194/hess-21-4615-2017>,  
785 2017.
- 786 Tan, H., Chen, J., Rao, W., Zhang, W., ~~& and~~ Zhou, H. (2012): Geothermal constraints on  
787 enrichment of boron and lithium in salt lakes: An example from a river-salt lake system on  
788 the northern slope of the eastern Kunlun Mountains, China ~~-, J. Asian. Earth. Sci.~~ ~~Journal of~~  
789 ~~Asian Earth Sciences~~, 51, 21-29, <https://doi.org/10.1016/j.jseas.2012.03.002>, 2012.
- 790 Tan, H., Rao, W., Chen, J., Su, Z., Sun, X., ~~& and~~ Liu, X. (2009): Chemical and isotopic approach  
791 to groundwater cycle in western Qaidam Basin, China ~~-, Chinese. Geogr. Sci.~~ ~~Chinese~~  
792 ~~Geographical Science~~, 19, 357-364, <https://doi.org/10.1007/s11769-009-0357-9>, 2009.
- 793 Tan, H., Zhang, Y., Rao, W., Guo, H., Ta, W., Lu, S., ~~& and~~ Cong, P. (2021): Rapid groundwater  
794 circulation inferred from temporal water dynamics and isotopes in an arid system ~~-, Hydrol.~~  
795 ~~Process.~~ ~~Hydrological Processes~~, 35(6), e14225, <https://doi.org/10.1002/hyp.14225>, 2021.
- 796 Tian, L., Yao, T., Sun, W., Stievenard, M., ~~& and~~ Jouzel, J. (2001): Relationship between  $\delta D$  and  
797  $\delta^{18}O$  in precipitation on north and south of the Tibetan Plateau and moisture recycling ~~-, Sci.~~  
798 ~~China. Ser. D.~~ ~~Science in China Series D: Earth Sciences~~, 44(9), 789-796,  
799 <https://doi.org/10.1007/BF02907091>, 2001.
- 800 Wang, L., Yao, T., Chai, C., Cuo, L., Su, F., Zhang, F., Yao, Z., Zhang, Y., Li, X., Qi, J., Hu, Z.,  
801 Liu, J., ~~& and~~ Wang, Y. (2021): TP-River: Monitoring and Quantifying Total River Runoff  
802 from the Third Pole, ~~B. Am. Meteorol. Soc.~~ ~~Bulletin of the American Meteorological Society~~,  
803 102(5), E948-E965, <https://doi.org/10.1175/BAMS-D-20-0207.1>, 2021.
- 804 Wang, S., Lei, S., Zhang, M., Hughes, C., Crawford, J., Liu, Z., ~~& and~~ Qu, D. (2022): Spatial and  
805 seasonal isotope variability in precipitation across China: Monthly isoscapes based on  
806 regionalized fuzzy clustering ~~-, J. Climate.~~ ~~Journal of Climate~~, 35(11), 3411-3425,  
807 <https://doi.org/10.1175/JCLI-D-21-0451.1>, 2022.

- 808 Wang, S., Zhang, M., Che, Y., Chen, F., & Qiang, F. ~~(2016)~~: Contribution of recycled moisture  
809 to precipitation in oases of arid central Asia: A stable isotope approach. ~~Water Resour.~~  
810 ~~Res. Water Resources Research~~, 52(4), 3246-3257, <https://doi.org/10.1002/2015WR018135>,  
811 ~~2016~~.
- 812 Wang, T., Yang, D., Yang, Y., Zheng, G., Jin, H., Li, X., ~~Yao, T., & Cheng, G.~~ ~~(2023)~~:  
813 Unsustainable water supply from thawing permafrost on the Tibetan Plateau in a changing  
814 climate. ~~Sci. Bull. Science bulletin~~, S2095-9273, <https://doi.org/10.1016/j.scib.2023.04.037>,  
815 ~~2023~~.
- 816 Wang, X., Chen, M., Gong, P., ~~& Wang, C.~~ ~~(2019)~~: Perfluorinated alkyl substances in snow  
817 as an atmospheric tracer for tracking the interactions between westerly winds and the Indian  
818 Monsoon over western China. ~~Environ. Int. Environment international~~, 124, 294-301,  
819 <https://doi.org/10.1016/j.envint.2018.12.057>, 2019.
- 820 Wang, X., Yang, M., Liang, X., Pang, G., Wan, G., Chen, X., ~~& Luo, X.~~ ~~(2014)~~: The dramatic  
821 climate warming in the Qaidam Basin, northeastern Tibet Plateau, during 1961–2010. ~~Int. J.~~  
822 ~~Climatol. International Journal of Climatology~~, 34(5), 1524-1537,  
823 <https://doi.org/10.1002/joc.3781>, 2014.
- 824 Wang, Y., Guo, H., Li, J., Huang, Y., Liu, Z., Liu, C., Guo, X., Zhou, J., Shang, X., Li, J., Zhuang,  
825 Y., ~~& Cheng, H.~~ ~~(2008)~~. ~~(1st ed.)~~: Investigation and assessment of groundwater resources  
826 and their environmental issues in the Qaidam Basin. Geological Publishing House, Beijing,  
827 ~~447 pp, ISBN978-7-116-05909-2, 2008~~ (in Chinese).
- 828 Wei, L., Jiang, S., Ren, L., Tan, H., Ta, W., Liu, Y., ~~Yang, X., Zhang, L., & Duan, Z.~~ ~~(2021)~~:  
829 Spatiotemporal changes of terrestrial water storage and possible causes in the closed Qaidam  
830 Basin, China using GRACE and GRACE Follow-On data. ~~J. Hydrol. Journal of Hydrology~~,  
831 598, 126274, <https://doi.org/10.1016/j.jhydrol.2021.126274>, 2021.
- 832 Wen, G., Wang, W., Duan, L., Gu, X., Li, Y., ~~& Zhao, J.~~ ~~(2018)~~: Quantitatively evaluating  
833 exchanging relationship between river water and groundwater in Bayin River Basin of  
834 northwest China using hydrochemistry and stable isotope. ~~Arid Land Geography~~, 41(04),  
835 734-743, <https://doi.org/10.13826/j.cnki.cn65-1103/x.2018.04.008>, 2018 (in Chinese with  
836 English abstract).
- 837 Wu, H., Zhang, C., Li, XY, Fu, C., Wu, H., Wang, P., ~~& Liu, J.~~ ~~(2022)~~: Hydrometeorological  
838 Processes and Moisture Sources in the Northeastern Tibetan Plateau: Insights from a 7-Yr

839 Study on Precipitation Isotopes—, ~~Journal of~~ Climate., 35(20), ~~2919-2931~~6519-6531,  
840 <https://doi.org/10.1175/JCLI-D-21-0501.1>, 2022.

841 Xiang, L., Wang, H., Steffen, H., Wu, P., Jia, L., Jiang, L., ~~& and~~ Shen, Q. ~~(2016)~~: Groundwater  
842 storage changes in the Tibetan Plateau and adjacent areas revealed from GRACE satellite  
843 gravity data—, ~~Earth. Planet. Sci. Lett.~~Earth and Planetary Science Letters, 449, 228-239,  
844 <https://doi.org/10.1016/j.epsl.2016.06.002>, 2016.

845 Xiao, Y., Shao, J., Cui, Y., Zhang, G., ~~& and~~ Zhang, Q. ~~(2017)~~: Groundwater circulation and  
846 hydrogeochemical evolution in Nomhon of Qaidam Basin, northwest China—, ~~Journal of Earth~~  
847 ~~System Science~~, 126 ~~(2)~~, 1-16, <https://doi.org/10.1007/s12040-017-0800-8>, 2017.

848 Xiao, Y., Shao, J., Frapce, SK, Cui, Y., Dang, X., Wang, S., ~~& and~~ Ji, Y. ~~(2018)~~: Groundwater  
849 origin, flow regime and geochemical evolution in arid endorheic watersheds: a case study  
850 from the Qaidam Basin, northwestern China—, ~~Hydrol. Earth. Syst. Sci.~~Hydrology and Earth  
851 ~~System Sciences~~, 22(8), 4381-4400, <https://doi.org/10.5194/hess-22-4381-2018>, 2018.

852 Xu, W., Su, X., Dai, Z., Yang, F., Zhu, P., ~~& and~~ Huang, Y. ~~(2017)~~: Multi-tracer investigation of  
853 river and groundwater interactions: a case study in Nalenggele River basin, northwest China—,  
854 ~~Hydrogeol. J.~~Hydrogeology Journal, 25(7), 2015-2029, [https://doi.org/10.1007/s10040-017-](https://doi.org/10.1007/s10040-017-1606-0)  
855 [1606-0](https://doi.org/10.1007/s10040-017-1606-0), 2017.

856 Yang, N., ~~& and~~ Wang, G. ~~(2020)~~: Moisture sources and climate evolution during the last 30 kyr  
857 in northeastern Tibetan Plateau: Insights from groundwater isotopes (2H, 18O, 3H and 14C)  
858 and water vapor trajectories modeling—, ~~Quaternary. Sci. Rev.~~Quaternary Science Reviews,  
859 242, 106426, <https://doi.org/10.1016/j.quascirev.2020.106426>, 2020.

860 Yang, N., Wang, G., Liao, F., Dang, X., ~~& and~~ Gu, X. ~~(2023)~~: Insights into moisture sources and  
861 evolution from groundwater isotopes (2H, 18O, and 14C) in Northeastern Qaidam Basin,  
862 Northeast Tibetan Plateau, China—, ~~Sci. Total. Environ.~~Science of The Total Environment,  
863 864, 160981, <https://doi.org/10.1016/j.scitotenv.2022.160981>, 2023.

864 Yang, N., Zhou, P., Wang, G., Zhang, B., Shi, Z., Liao, F., ~~Li, B., Chen, X., Guo, L., Dang, X.,~~  
865 ~~& and~~ Gu, X. ~~(2021)~~: Hydrochemical and isotopic interpretation of interactions between  
866 surfaces water and groundwater in Delingha, Northwest China—, ~~J. Hydrol.~~Journal of  
867 ~~Hydrology~~, 598, 126243, <https://doi.org/10.1016/j.jhydrol.2021.126243>, 2021.

868 Yang, Y., Wu, Q., & Jin, H. (2016): Evolutions of water stable isotopes and the contributions  
869 of cryosphere to the alpine river on the Tibetan Plateau, *Environ. Earth Sci. Environmental*  
870 *Earth Sciences*, 75(1), 1-11, <https://doi.org/10.1007/s12665-015-4894-5>, 2016.

871 Yao, T., Bolch, T., Chen, D., Gao, J., Immerzeel, W., Piao, S., Su, F., Thompson, L., Wada, Y.,  
872 Wang, L., Wang, T., Wu, G., Xu, B., Yang, W., Zhang, G., ... & Zhao, P. (2022): The  
873 imbalance of the Asian water tower, *Nat. Rev. Earth. Env. Nature Reviews Earth &*  
874 *Environment*, 1-15 <https://doi.org/10.1038/s43017-022-00299-4>, 2022.

875 Yao, T., Masson-Delmotte, V., Gao, J., Yu, W., Yang, X., Risi, C., Sturm, C., Werner, M., Zhao,  
876 H., He, Y., Ren, W., Tian, L., Shi, C., ... & Hou, S. (2013): A review of climatic controls  
877 on  $\delta^{18}\text{O}$  in precipitation over the Tibetan Plateau: Observations and simulations, *Rev.*  
878 *Geophys. Reviews of Geophysics*, 51(4), 525-548, <https://doi.org/10.1002/rog.20023>, 2013.

879 Ye, C., Zheng, M., Wang, Z., Hao, W., Wang, J., Lin, X., & Han, J. (2015): Hydrochemical  
880 characteristics and sources of brines in the Gasikule salt lake, Northwest Qaidam Basin,  
881 China, *Geochem. J. Geochemical Journal*, 49(5), 481-494,  
882 <https://doi.org/10.2343/geochemj.2.0372>, 2015.

883 Zhang, G., Yao, T., Shum, C. K., Yi, S., Yang, K., Xie, H., Feng, W., Bolch, T., Wang, L., Behrangi,  
884 A., Zhang, H., Wang, W., Xiang, Y., ... & Yu, J. (2017): Lake volume and groundwater  
885 storage variations in Tibetan Plateau's endorheic basin, *Geophys. Res. Lett. Geophysical*  
886 *Research Letters*, 44(11), 5550-5560, <https://doi.org/10.1002/2017GL073773>, 2017.

887 Zhang, Q., Zhu, B., Yang, J., Ma, P., Liu, X., Lu, G., Wang, Y., Yu, H., Liu, W., ... & Wang,  
888 D. (2021): New characteristics about the climate humidity trend in Northwest China,  
889 *Chinese. Sci. Bull. Chinese Science Bulletin*, 66 (28-29), 3757-3771,  
890 <https://doi.org/10.1360/TB-2020-1396>, 2021.

891 Zhang, X., Chen, J., Chen, J., Ma, F., & Wang, T. (2022): Lake Expansion under the  
892 Groundwater Contribution in Qaidam Basin, China, *Remote. Sens. Remote Sensing*,  
893 14(7), 1756, <https://doi.org/10.3390/rs14071756>, 2022.

894 Zhao, D., Wang, G., Liao, F., Yang, N., Jiang, W., Guo, L., Liu, C., ... & Shi, Z. (2018):  
895 Groundwater-surface water interactions derived by hydrochemical and isotopic ( $^{222}\text{Rn}$ ,  
896 deuterium, oxygen-18) tracers in the Nomhon area, Qaidam Basin, NW China, *J.*  
897 *Hydrol. Journal of Hydrology*, 565, 650-661, <https://doi.org/10.1016/j.jhydrol.2018.08.066>,  
898 2018.



- 899 Zhao, L., Yin, L., Xiao, H., Cheng, G., Zhou, M., Yang, Y., Li, C., ... & Zhou, J. ~~(2011)~~:  
900 Isotopic evidence for the moisture origin and composition of surface runoff in the headwaters  
901 of the Heihe River basin-, Chinese. Sci. Bull.Chinese Science Bulletin, 56(4), 406-415,  
902 <https://doi.org/10.1007/s11434-010-4278-x>, 2011.
- 903 Zhu, G., Liu, Y., Wang, L., Sang, L., Zhao, K., Zhang, Z., Lin, X., ... & Qiu, D. ~~(2023)~~: The  
904 isotopes of precipitation have climate change signal in arid Central Asia-, Global. Planet.  
905 Change.Global and Planetary Change, 225, 104103,  
906 <https://doi.org/10.1016/j.gloplacha.2023.104103>, 2023.
- 907 Zhu, J., Chen, H., & Gong, G. ~~(2015)~~: Hydrogen and oxygen isotopic compositions of  
908 precipitation and its water vapor sources in Eastern Qaidam Basin-, Environmental Science,  
909 36(8), 2784-2790, <https://doi.org/10.13227/j.hjcx.2015.08.008>, 2015 (in Chinese with  
910 English abstract).
- 911 Zhu, P. ~~(2015)~~: Groundwater circulation patterns of Yuqia-Maihai Basin in the middle and lower  
912 reaches of Yuqia River-, Ph.D. thesisDoctoral dissertation, Jilin University, Changchun, 2015  
913 (in Chinese with English abstract).
- 914 Zou, Y., Kuang, X., Feng, Y., Jiao, J., Liu, J., Wang, C., Fan, L., Wang, Q., Chen, J., Ji, F., Yao,  
915 Y., ... & Zheng, C. ~~(2022)~~: Solid water melt dominates the increase of total groundwater  
916 storage in the Tibetan Plateau-, Geophys. Res. Lett.Geophysical Research Letters,  
917 e2022GL100092, <https://doi.org/10.1029/2022GL100092>, 2022.